E

F

G

A B C D E F G H G F E D C B A

G

F

E

Atomistic simulation studies in the C/Si system

Frank Zirkelbach

Application talk at the Max Planck Institute for Solid State Research

Stuttgart, November 2011

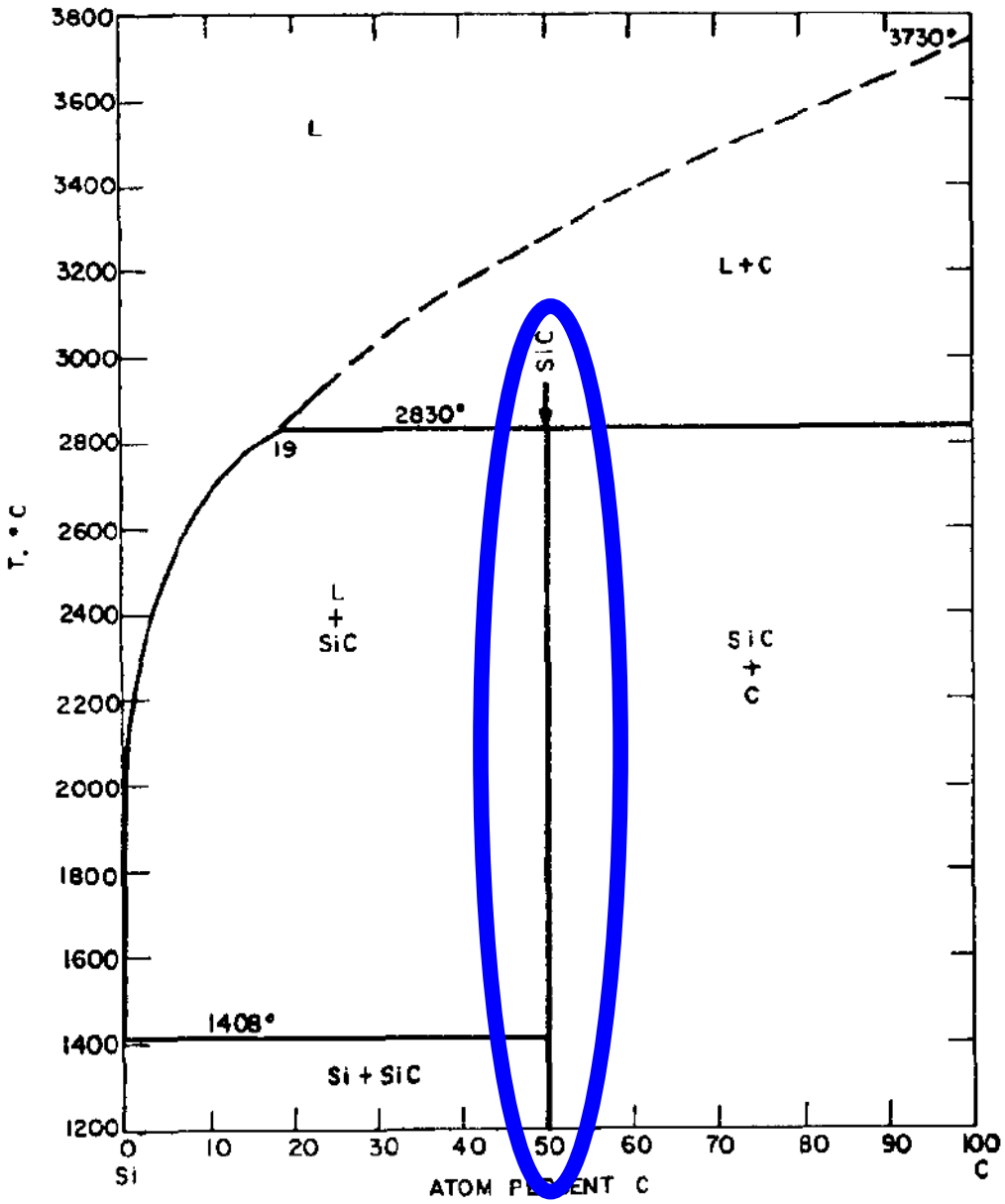

R. I. Scace and G. A. Slack, J. Chem. Phys. 30, 1551 (1959)

Phase diagram of the C/Si system

Stoichiometric composition

- only chemical stable compound
- wide band gap semiconductor silicon carbide, SiC

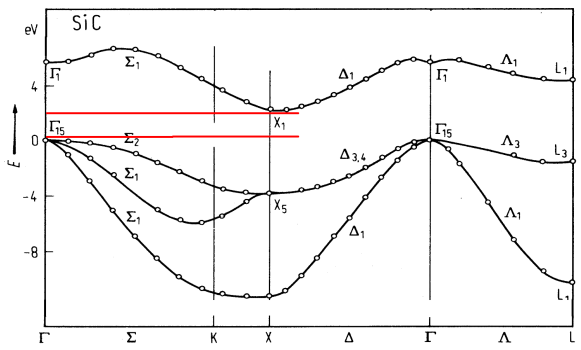

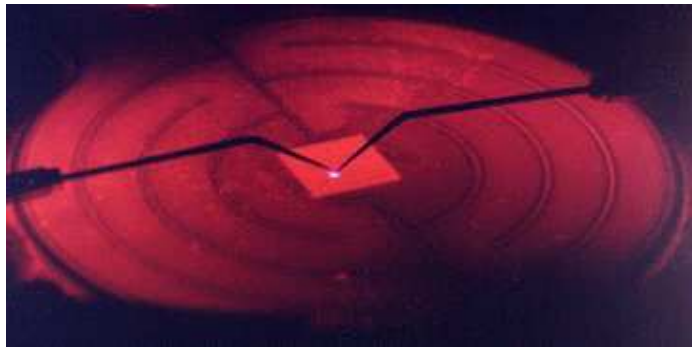

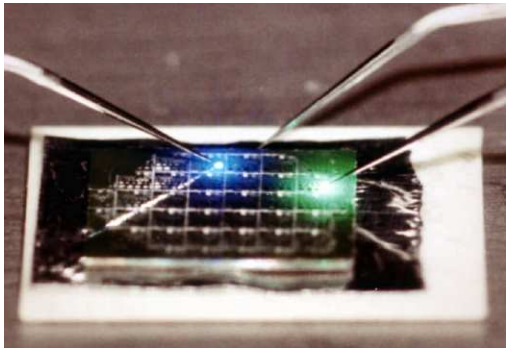

PROPERTIES

wide band gap

high electric breakdown field

good electron mobility

high electron saturation drift velocity

high thermal conductivity

hard and mechanically stable

chemically inert

radiation hardness

APPLICATIONS

high-temperature, high power
and high-frequency
electronic and optoelectronic devices

material suitable for extreme conditions
microelectromechanical systems
abrasives, cutting tools, heating elements

first wall reactor material, detectors
and electronic devices for space

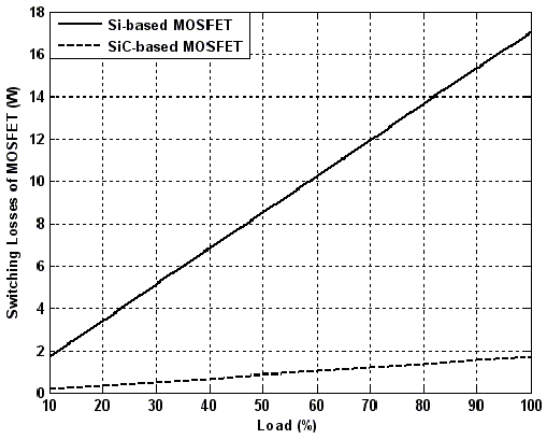

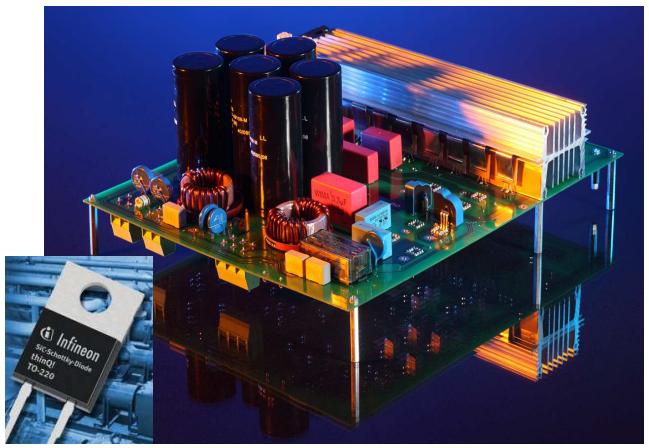

Polytypes of SiC

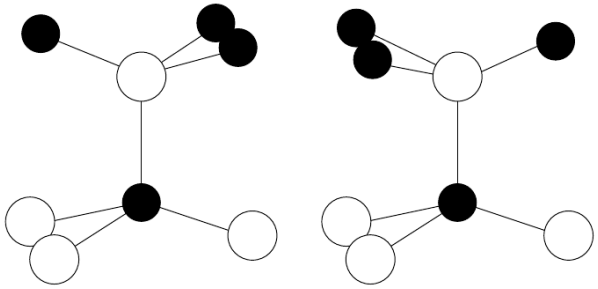

cubic (twist) hexagonal (no twist)

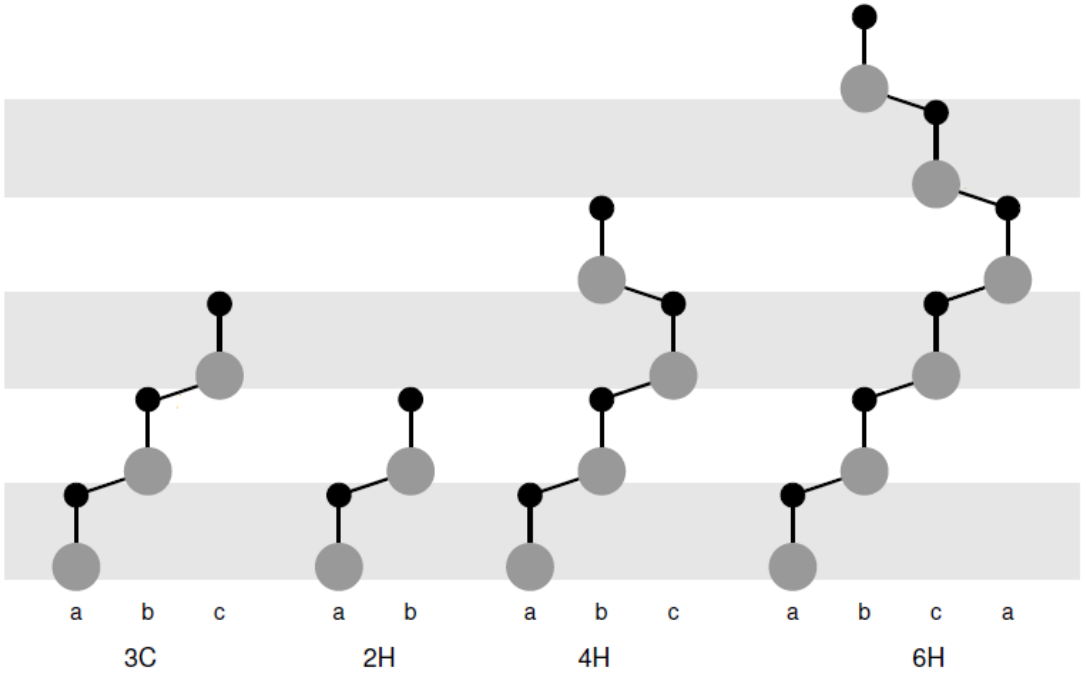

	3C-SiC	4H-SiC	6H-SiC	Si	GaN	Diamond
Hardness [Mohs]		—— 9.6 ——		6.5	-	10
Band gap [eV]	2.36	3.23	3.03	1.12	3.39	5.5
Break down field [10^6 V/cm]	4	3	3.2	0.6	5	10
Saturation drift velocity [10^7 cm/s]	2.5	2.0	2.0	1	2.7	2.7
Electron mobility [cm^2/Vs]	800	900	400	1100	900	2200
Hole mobility [cm^2/Vs]	320	120	90	420	150	1600
Thermal conductivity [W/cmK]	5.0	4.9	4.9	1.5	1.3	22

Fabrication of silicon carbide

Silicon carbide — Born from the stars, perfected on earth.

SiC thin films by MBE & CVD

- Much progress achieved in homo/heteroepitaxial SiC thin film growth
- Commercially available semiconductor power devices based on α-SiC
- Production of favored 3C-SiC material less advanced
- Quality and size not yet sufficient

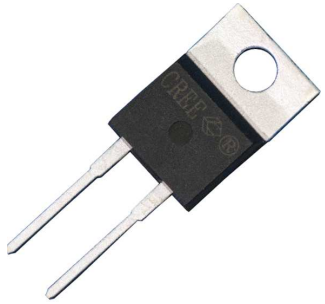

Alternative approach: Ion beam synthesis (IBS) of burried 3C-SiC layers in Si(1 0 0)

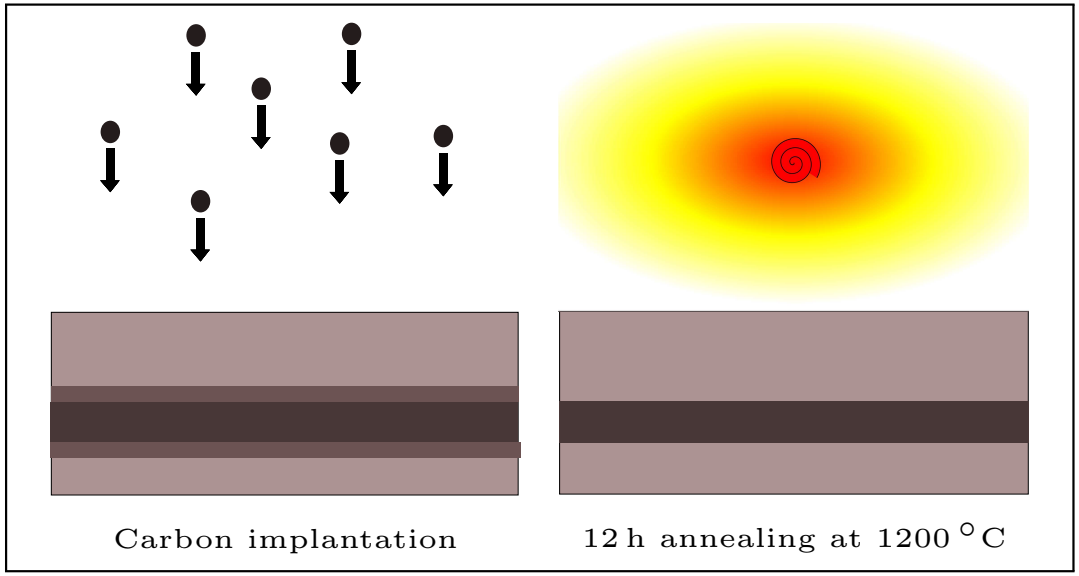

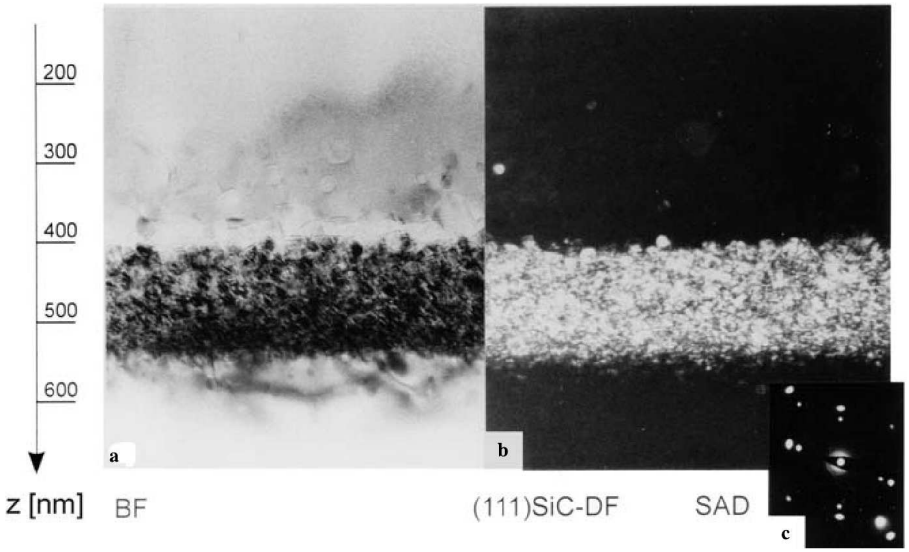

XTEM: single crystalline 3C-SiC in Si(1 0 0)

Systematic investigation of C implantations into Si

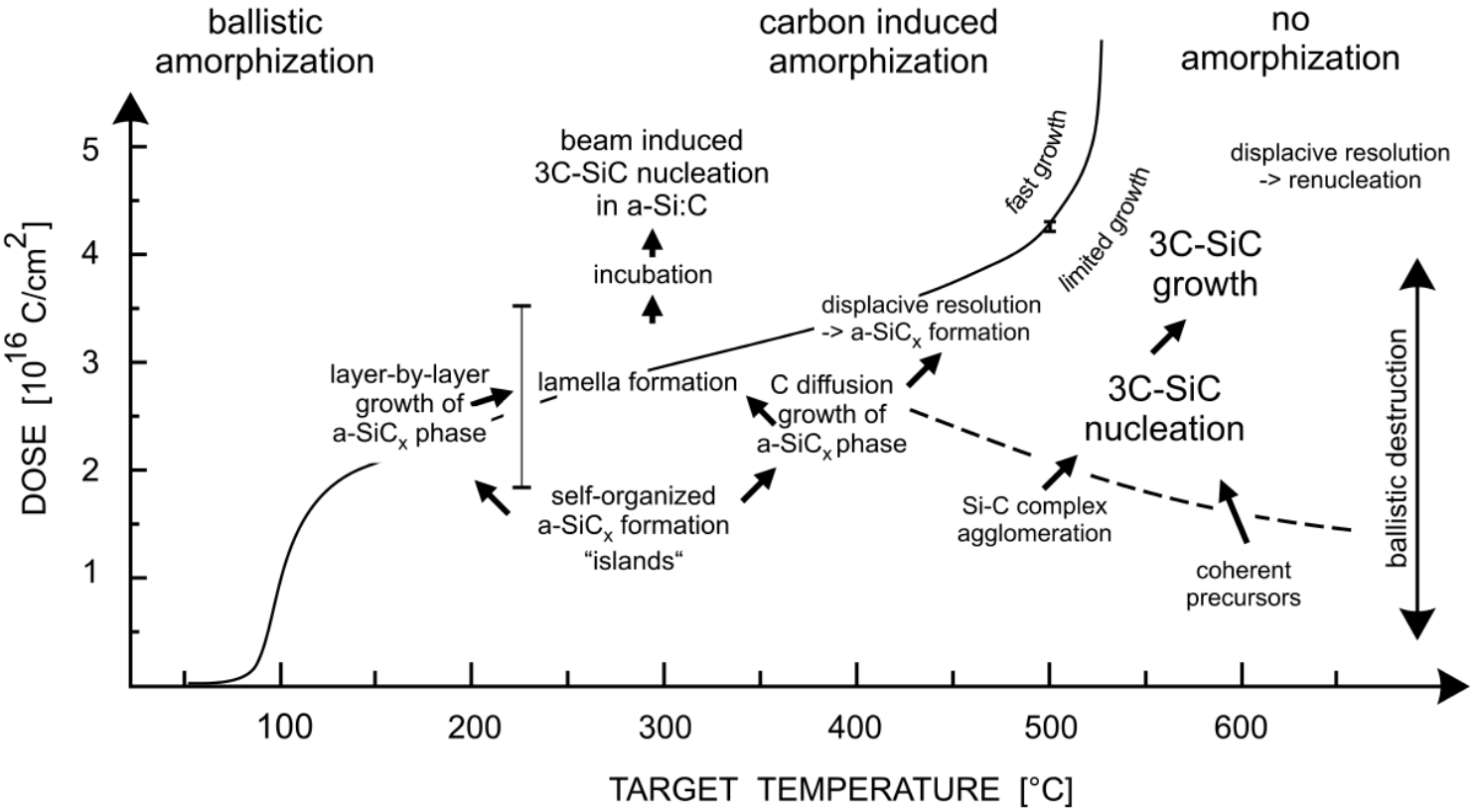

Outline

Diploma thesis

Monte Carlo simulation modeling the selforganization process leading to periodic arrays of nanometric amorphous SiC precipitates

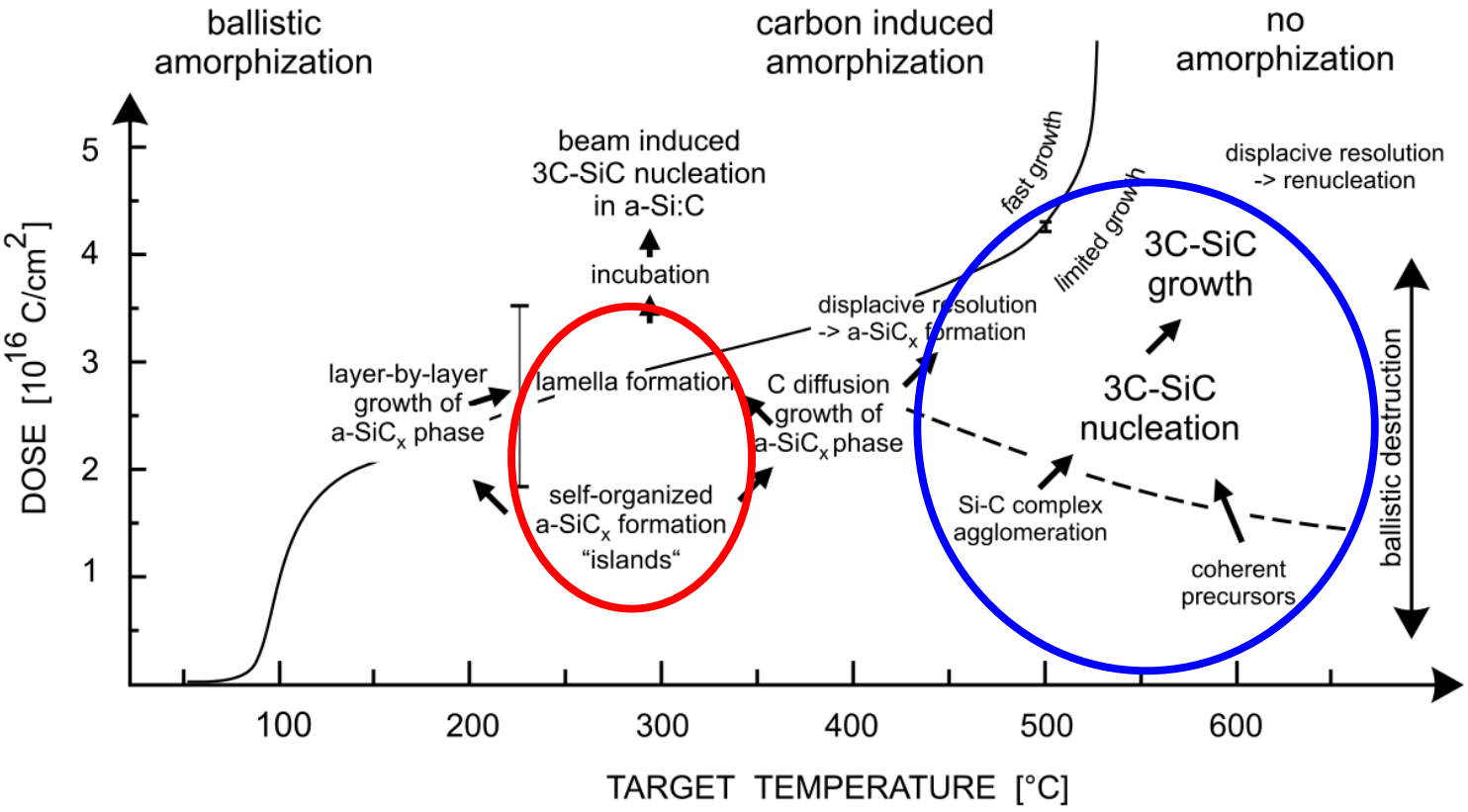

Doctoral studies

Classical potential molecular dynamics simulations ...

Density functional theory calculations ...

... on defect formation and SiC precipitation in Si

Selforganization of nanometric amorphous SiC lamellae

- Regularly spaced, nanometric spherical and lamellar amorphous inclusions at the upper a/c interface
- Carbon accumulation in amorphous volumes

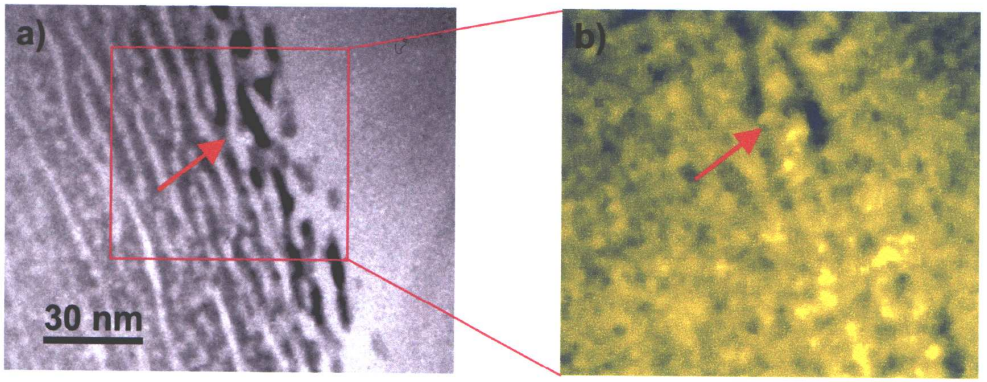

XTEM bright-field and respective EFTEM C map

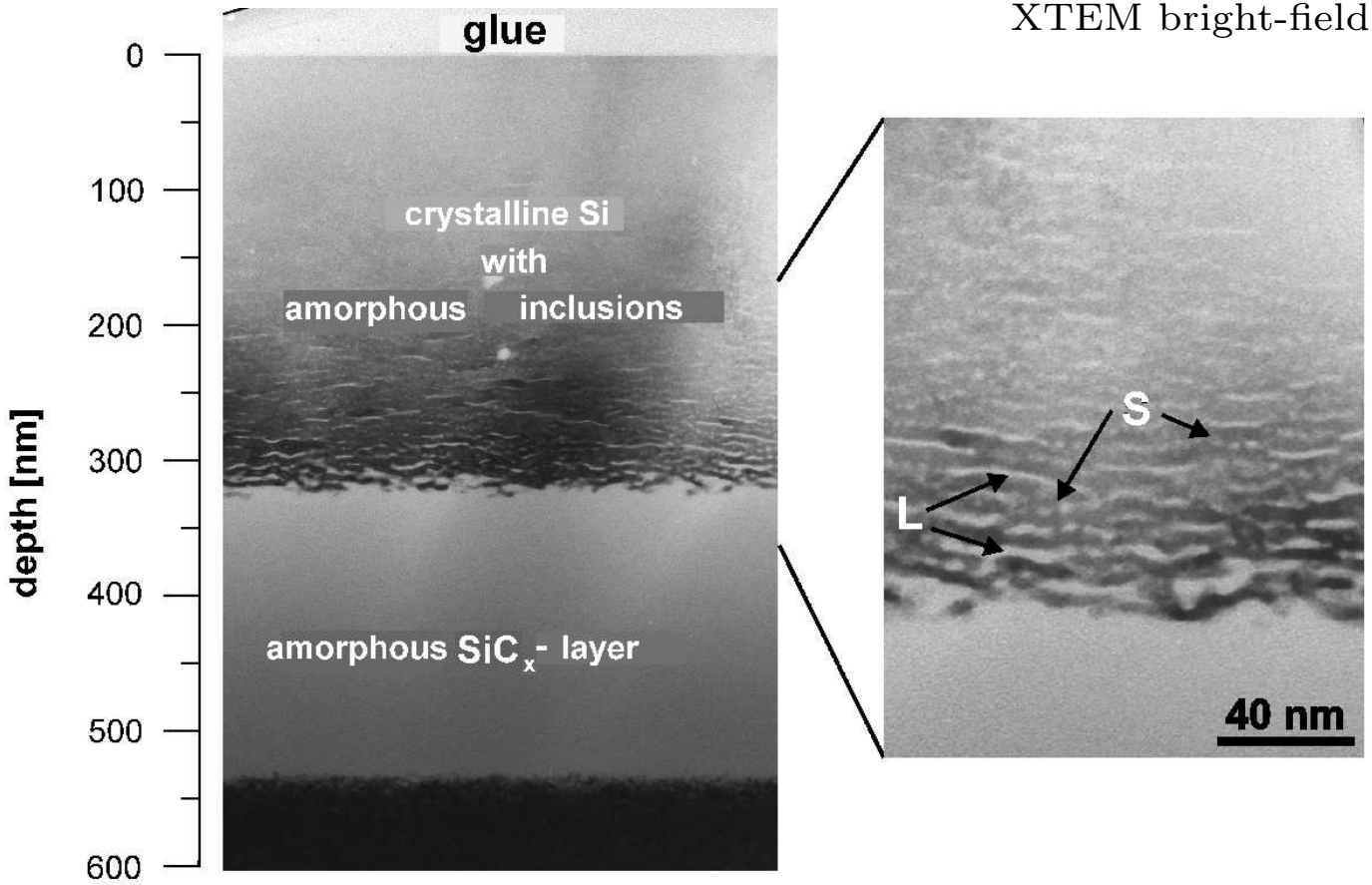

XTEM bright-field, 180 keV $C^+ \rightarrow$ Si, 150 °C, Dose: 4.3 $\times 10^{17}$ cm^{-2}

Model displaying the formation of ordered lamellae

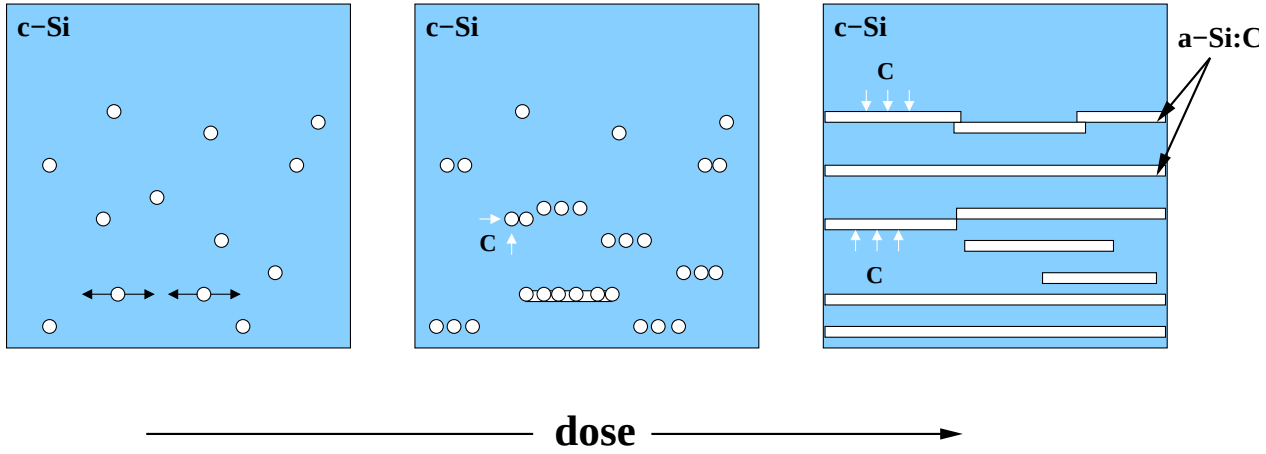

- Supersaturation of C in c-Si
  → **Carbon induced** nucleation of spherical SiC_x-precipitates
- High interfacial energy between 3C-SiC and c-Si
  → **Amorphous** precipitates
- 20– 30 % lower silicon density of a-SiC_x compared to c-Si
  → **Lateral strain** (black arrows)
- Implantation range near surface
  → **Relaxation** of **vertical strain component**
- Reduction of the carbon supersaturation in c-Si
  → **Carbon diffusion** into amorphous volumina (white arrows)
- Remaining lateral strain
  → **Strain enhanced** lateral amorphisation
- Absence of crystalline neighbours (structural information)
  → **Stabilization** of amorphous inclusions **against recrystallization**

Implementation of the Monte Carlo code

1. Amorphization / Recrystallization

   Ion collision in discretized target determined by random numbers distributed according to nuclear energy loss. Amorphization/recrystallization probability:

$$p_{c\to a}(\vec{r}) = p_b + p_c c_C(\vec{r}) + \sum_{\text{amorphous neighbours}} \frac{p_s c_C(\vec{r'})}{(r-r')^2}$$

   - p_b normal 'ballistic' amorphization
   - p_c carbon induced amorphization
   - p_s stress enhanced amorphization

$$p_{a\to c}(\vec{r}) = (1 - p_{c\to a}(\vec{r}))\left(1 - \frac{\sum_{direct\,neighbours}\delta(\vec{r'})}{6}\right),$$

$$\delta(\vec{r}) = \begin{cases} 1 & \text{if volume at position } \vec{r} \text{ is amorphous} \\ 0 & \text{otherwise} \end{cases}$$

2. Carbon incorporation

   Incorporation volume determined according to implantation profile

3. Diffusion / Sputtering

   - Transfer fraction of C atoms of crystalline into neighbored amorphous volumes
   - Remove surface layer

Results

Evolution of the . . .

- continuous amorphous layer
- a/c interface
- lamellar precipitates

. . . reproduced!

Experiment & simulation in good agreement

Simulation is able to model the whole depth region

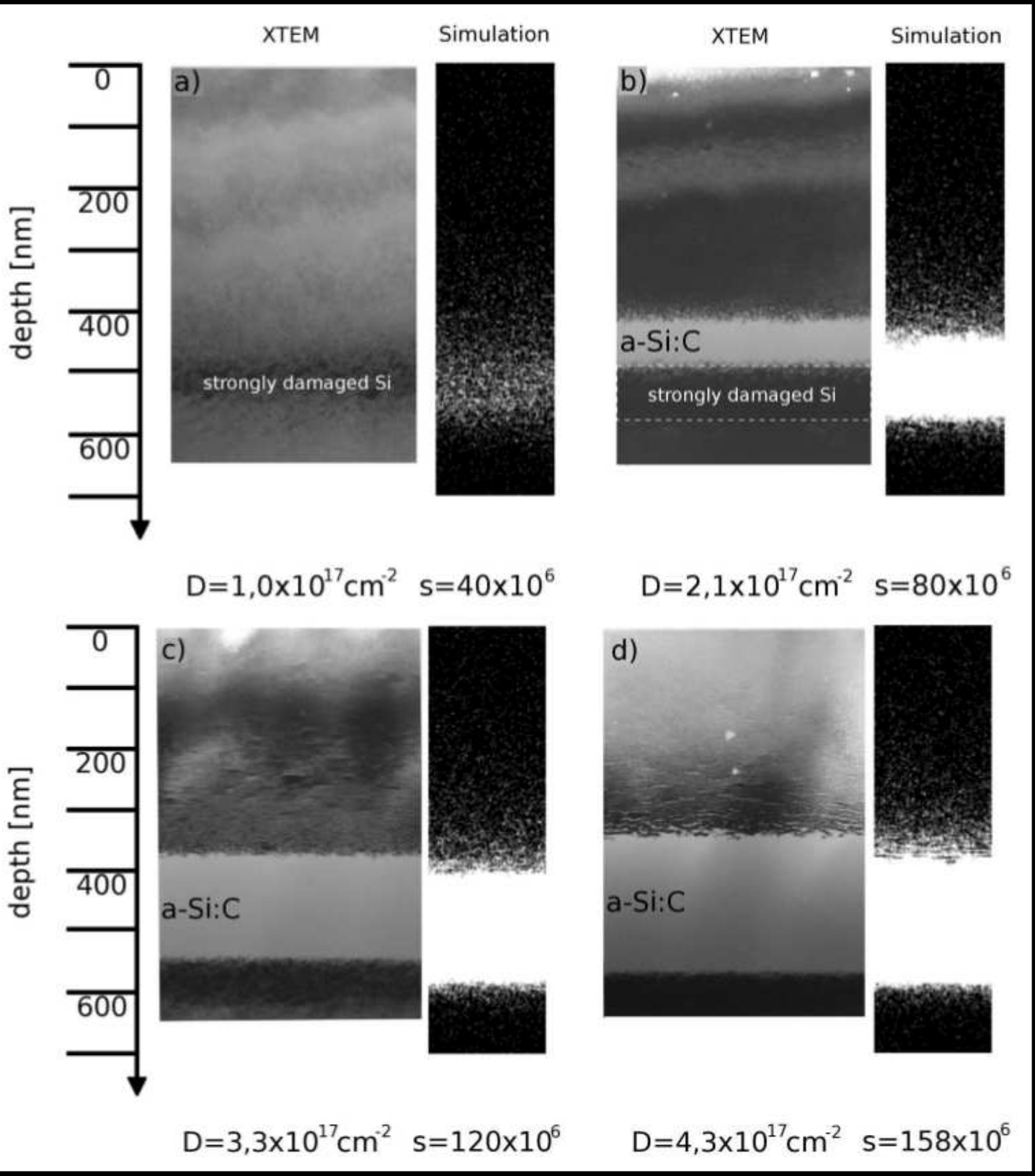

Structural & compositional details

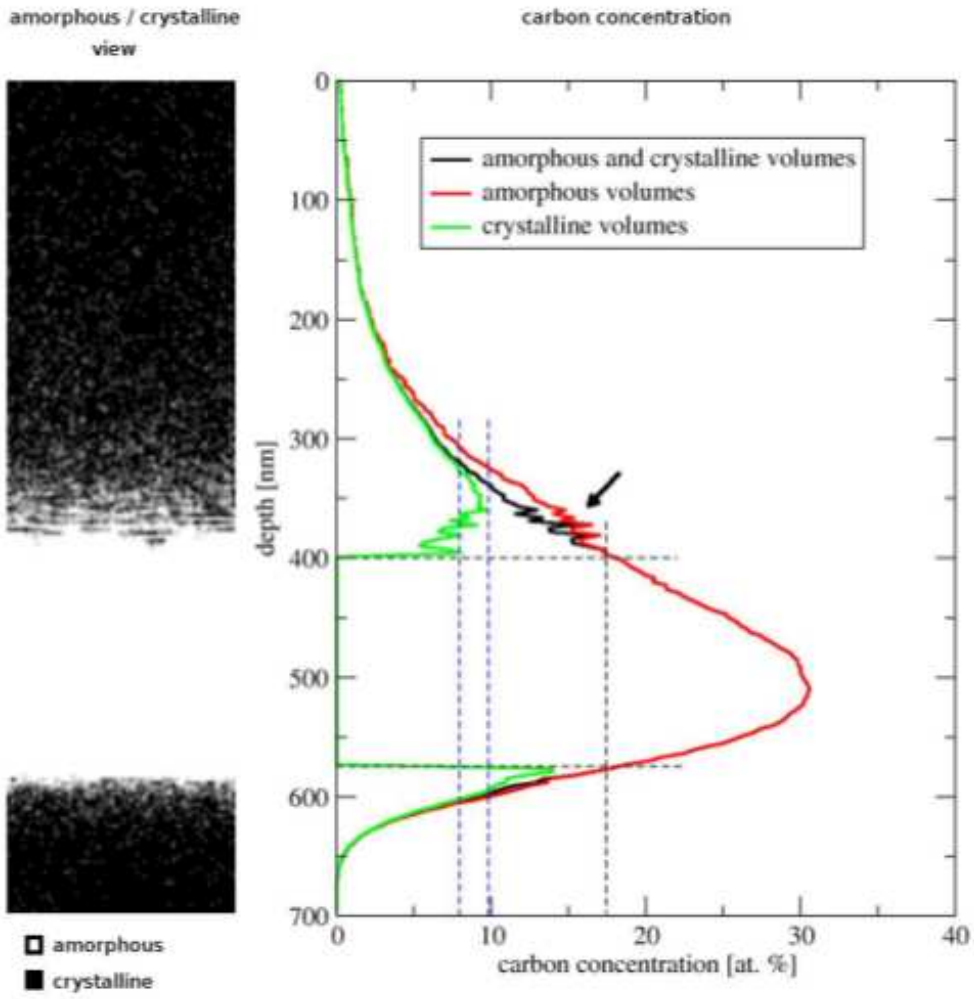

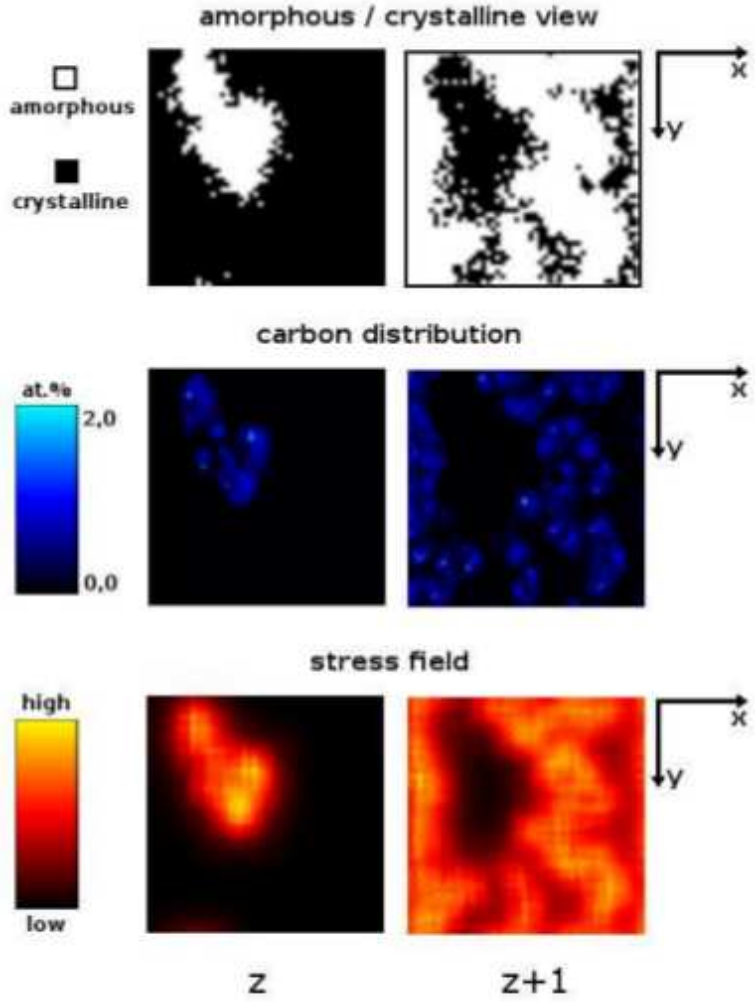

- Fluctuation of C concentration in lamellae region
- 8–10 at.% C saturation limit within the respective conditions
- Complementarily arranged and alternating sequence of layers with a high and low amount of amorphous regions
- C accumulation in the amorphous phase / Origin of stress

Precipitation process gets traceable by simulation!

Formation of epitaxial single crystalline 3C-SiC

- Implantation step 1

  Almost stoichiometric dose | 180 keV | 500 °C

  ⇒ Epitaxial 3C-SiC layer & precipitates

- Implantation step 2

  Little remaining dose | 180 keV | 250 °C

  ⇒ Destruction/Amorphization of precipitates at layer interface

- Annealing

  10 h at 1250 °C

  ⇒ Homogeneous 3C-SiC layer with sharp interfaces

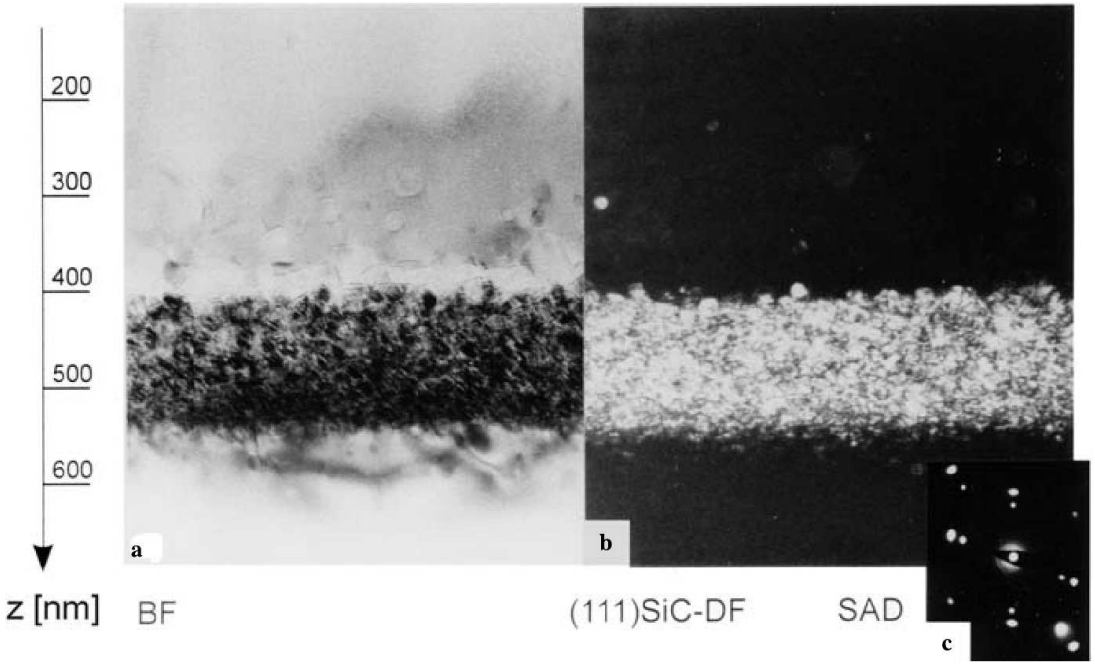

3C-SiC precipitation
not yet fully understood

Details of the SiC precipitation

⇒ significant technological progress in SiC thin film formation

⇒ perspectives for processes relying upon prevention of SiC precipitation

Supposed precipitation mechanism of SiC in Si

Si & SiC lattice structure

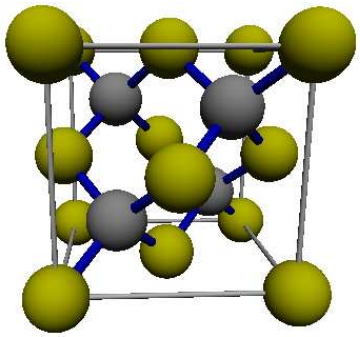

Silicon	Silicon carbide
• Si | • Si	• Si | • C
$a = 5.429$ A	$a = 4.359$ A
$\rho^*_{\mathrm{Si}} = 100\,\%$	$\rho^*_{\mathrm{Si}} = 97\,\%$

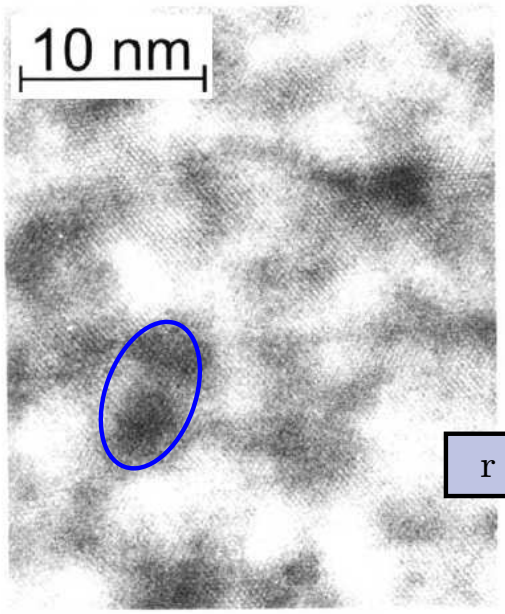

r = 2–4 nm

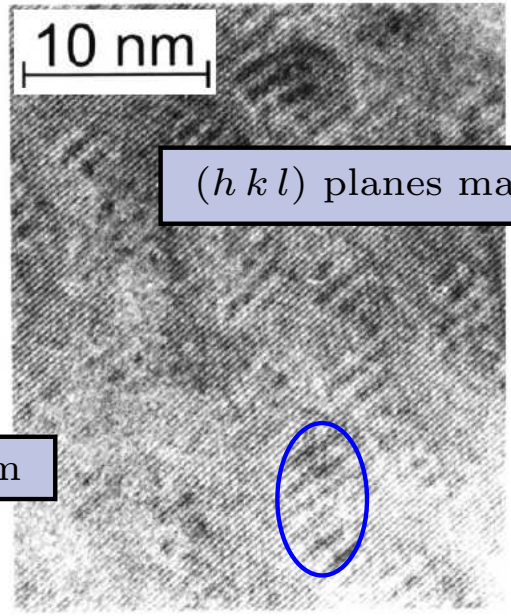

$(h\,k\,l)$ planes match

C-Si dimers (dumbbells)
on Si interstitial sites

Agglomeration of C-Si dumbbells
⇒ dark contrasts

Precipitation of 3C-SiC in Si
⇒ Moiré fringes
& release of Si self-interstitials

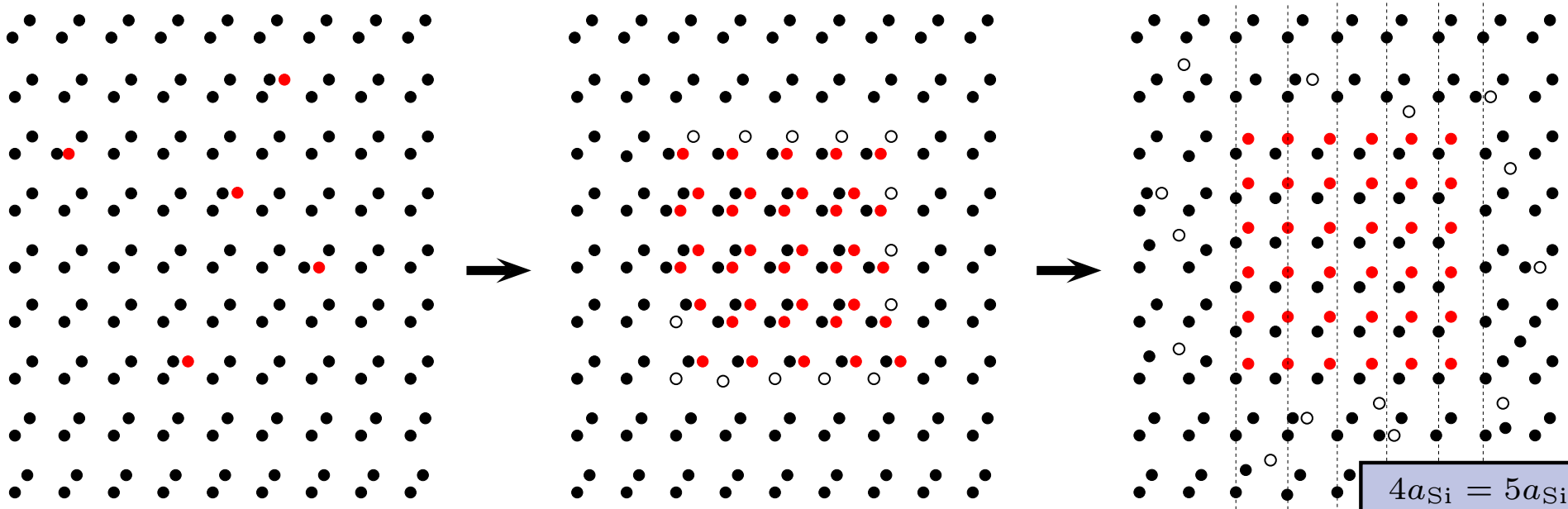

$4a_{\mathrm{Si}} = 5a_{\mathrm{SiC}}$

Supposed precipitation mechanism of SiC in Si

Controversial findings

- High-temperature implantation /Nejim et al./
  - C incorporated substitutionally on regular Si lattice sites
  - Si_i reacting with further C in cleared volume
- Annealing behavior /Serre et al./
  - Room temperature implantation → high C diffusion
  - Elevated temperature implantation → no C redistribution

  ⇒ mobile C_i opposed to stable C_{sub} configurations
- Strained silicon & Si/SiC heterostructures /Strane et al./Guedj et al./
  - Coherent SiC precipitates (tensile strain)
  - Incoherent SiC (strain relaxation)

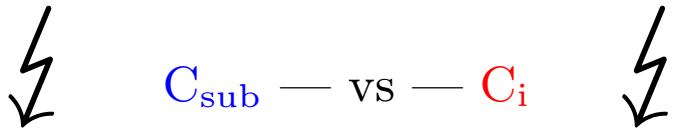

Utilized computational methods

Molecular dynamics (MD)

System of N particles	$N = 5832 \pm 1$ (Defects), $N = 238328 + 6000$ (Precipitation)
Phase space propagation	Velocity Verlet | timestep: 1 fs
Analytical interaction potential	Tersoff-like short-range, bond order potential (Erhart/Albe) $E = \frac{1}{2}\sum_{i \neq j} \mathcal{V}_{ij}, \quad \mathcal{V}_{ij} = f_C(r_{ij})\,[f_R(r_{ij}) + b_{ij}\, f_A(r_{ij})]$
Observables: time/ensemble averages	NpT (isothermal-isobaric) | Berendsen thermostat/barostat

Density functional theory (DFT)

- Hohenberg-Kohn theorem:
  $\Psi_0(r_1, r_2, \ldots, r_N) = \Psi[n_0(r)]$, $E_0 = E[n_0]$
- Kohn-Sham approach:
  Single-particle effective theory

- Code: VASP
- Plane wave basis set
- Ultrasoft pseudopotential
- Exchange & correlation: GGA
- Brillouin zone sampling: Γ-point
- Supercell: $N = 216 \pm 2$

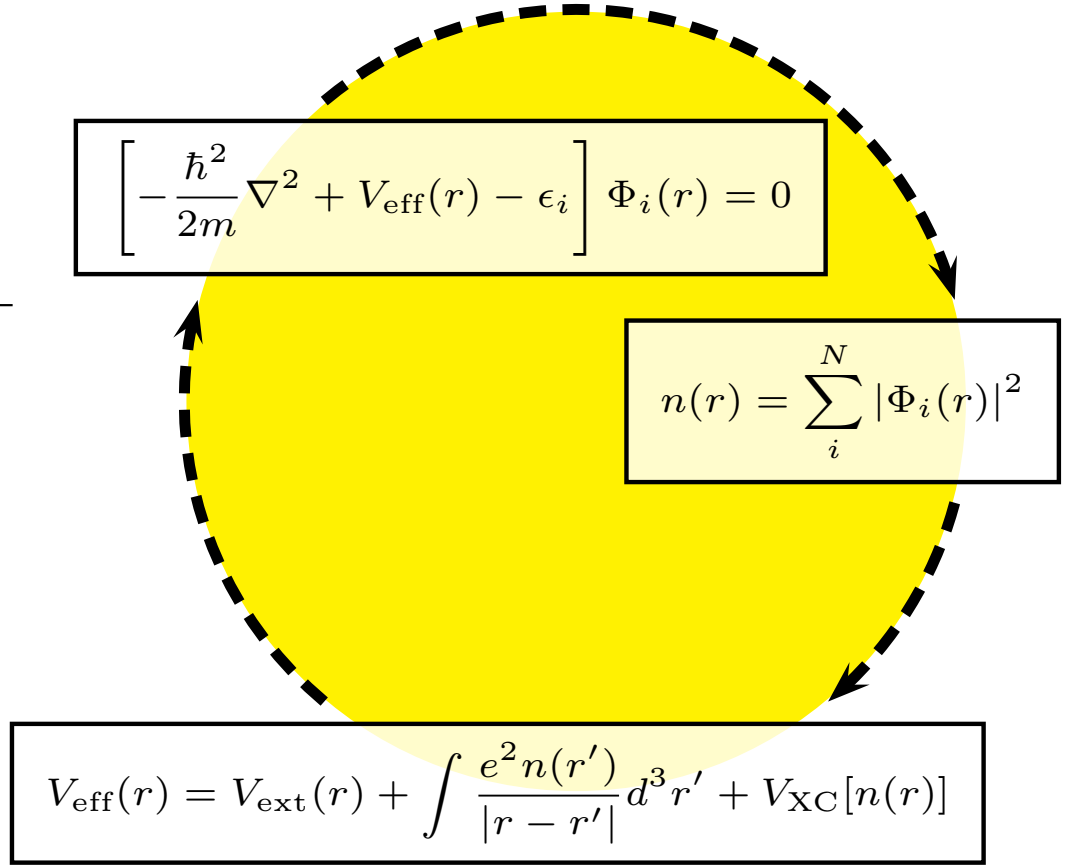

Point defects & defect migration

Defect structure

- Creation of c-Si simulation volume
- Periodic boundary conditions
- $T = 0$ K, $p = 0$ bar

↓

Insertion of interstitial C/Si atoms

↓

Relaxation / structural energy minimization

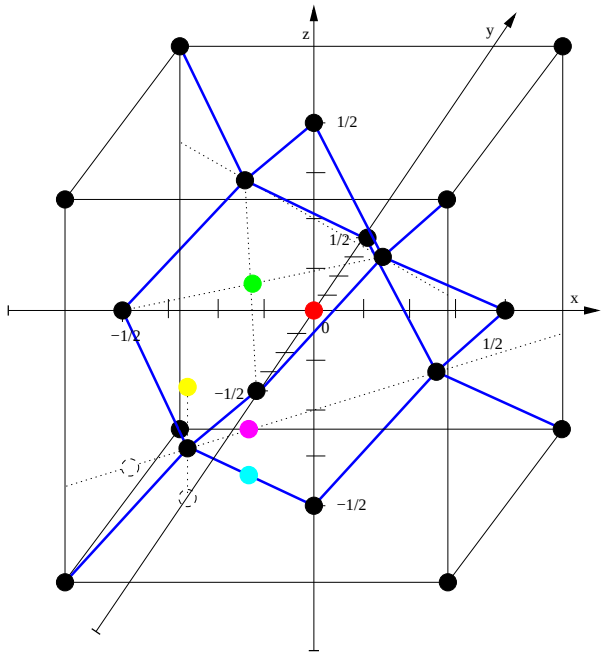

- Tetrahedral
- Hexagonal
- ⟨1 0 0⟩ DB
- ⟨1 1 0⟩ DB
- Bond-centered
- Vac. / Sub.

Defect formation energy

$$E_\mathrm{f} = E - \sum_i N_i \mu_i$$

Particle reservoir: Si & SiC

Binding energy

$$E_\mathrm{b} = E_\mathrm{f}^\mathrm{comb} - E_\mathrm{f}^{1^\mathrm{st}} - E_\mathrm{f}^{2^\mathrm{nd}}$$

$E_\mathrm{b} < 0$: energetically favorable configuration

$E_\mathrm{b} \to 0$: non-interacting, isolated defects

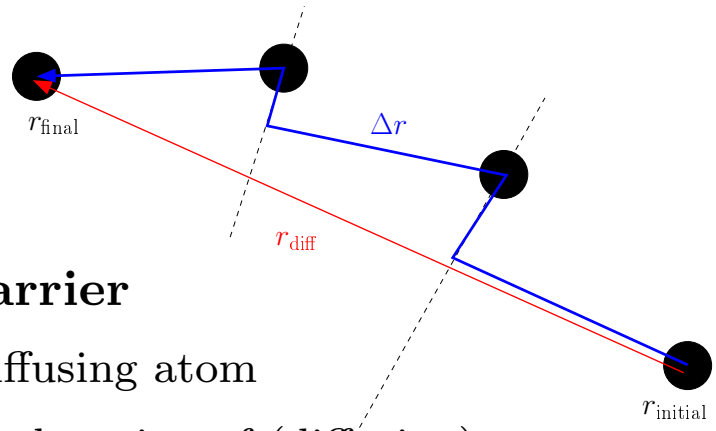

Migration barrier

- Displace diffusing atom
- Constrain relaxation of (diffusing) atoms
- Record configurational energy

Si self-interstitial point defects in silicon

E_f [eV]	$\langle 1\,1\,0\rangle$ DB	H	T	$\langle 1\,0\,0\rangle$ DB	V
VASP	3.39	3.42	3.77	4.41	3.63
Erhart/Albe	4.39	4.48*	3.40	5.42	3.13

Vacancy

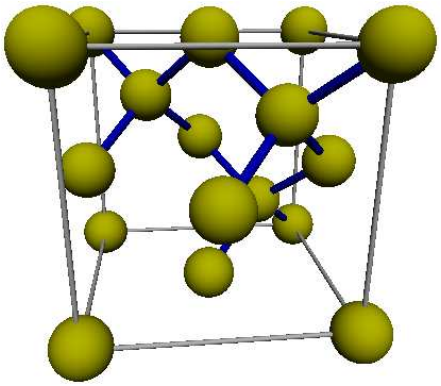

$\langle 1\,1\,0\rangle$ DB

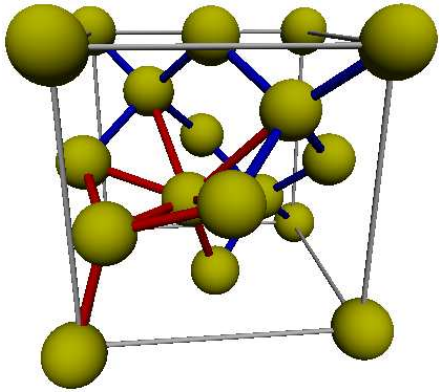

$\langle 1\,0\,0\rangle$ DB

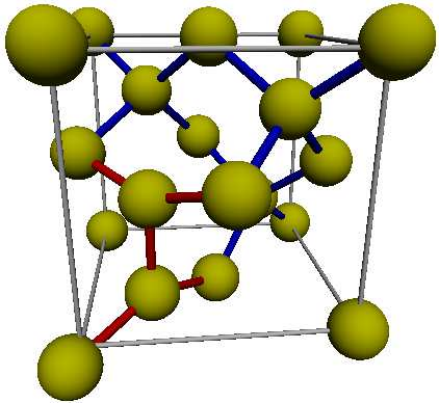

Tetrahedral

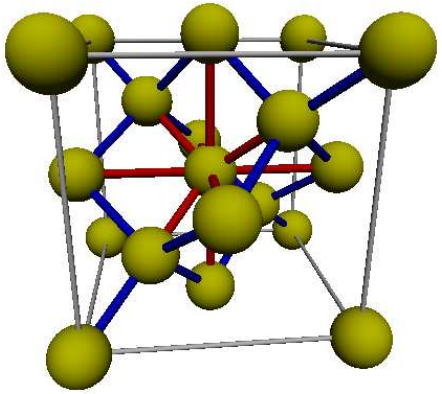

Hexagonal ▷

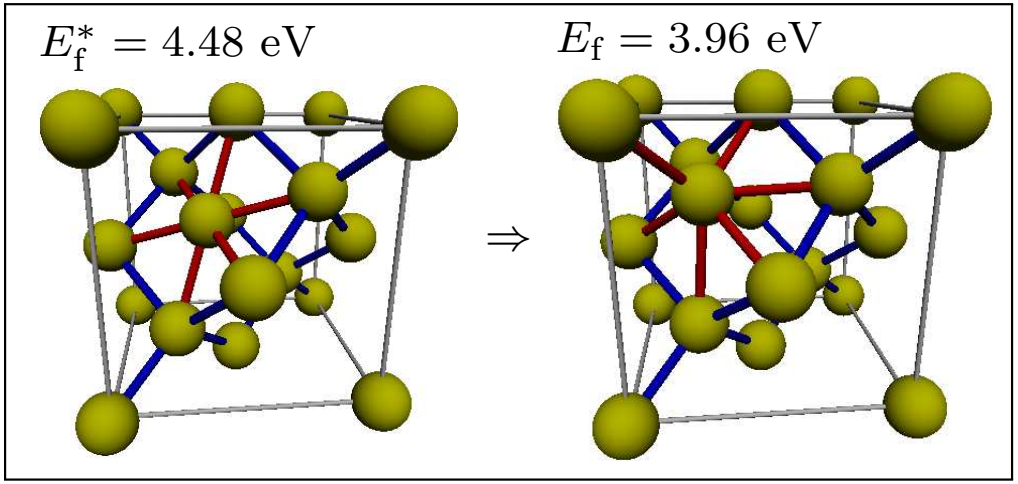

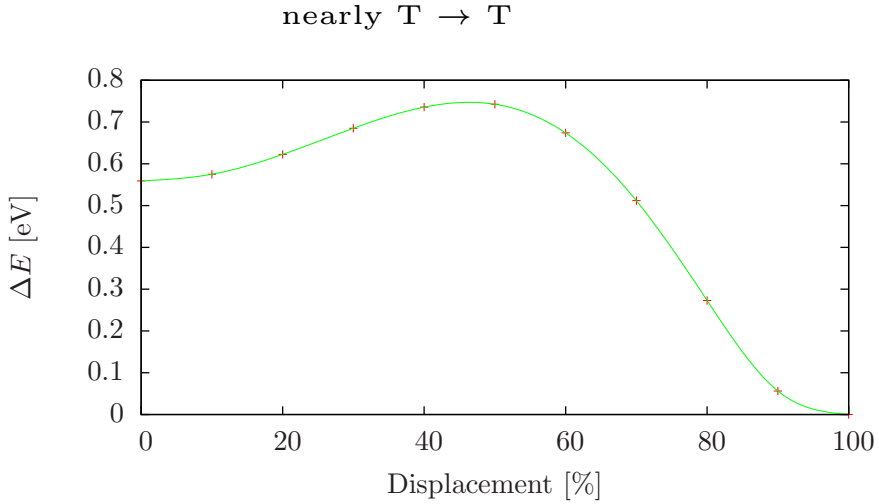

C interstitial point defects in silicon

E_f [eV]	T	H	⟨1 0 0⟩ DB	⟨1 1 0⟩ DB	S	B	C_{sub} & Si_i
VASP	unstable	unstable	3.72	4.16	1.95	4.66	4.17
Erhart/Albe	6.09	9.05*	3.88	5.18	0.75	5.59*	4.43

Hexagonal ▷
$E_f^* = 9.05$ eV

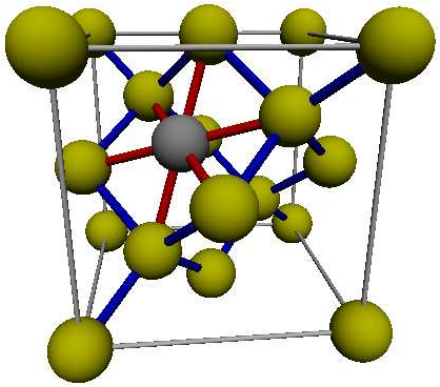

⇒

⟨1 0 0⟩
$E_f = 3.88$ eV

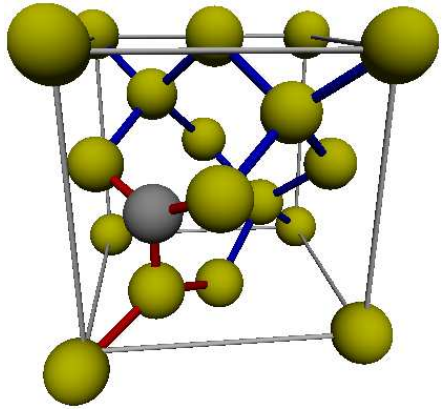

Tetrahedral

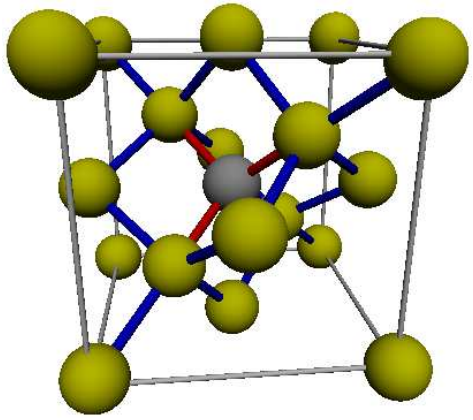

Bond-centered
$E_f^* = 5.59$ eV

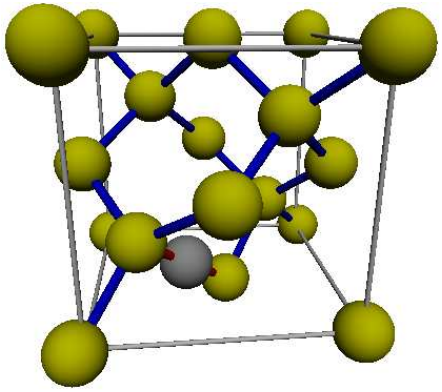

⇒

⟨1 1 0⟩ dumbbell
$E_f = 5.18$ eV

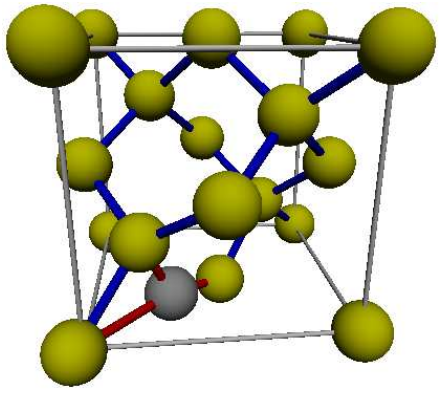

Substitutional

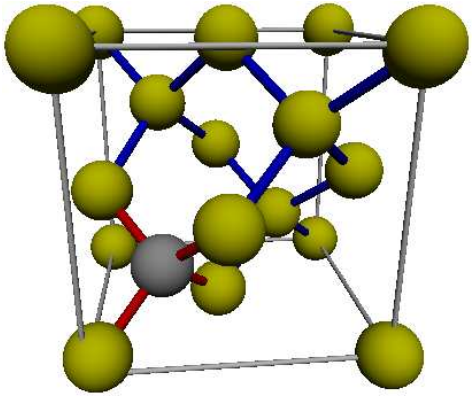

C-Si dimer & bond-centered interstitial configuration

C ⟨1 0 0⟩ DB interstitial

Erhart/Albe VASP

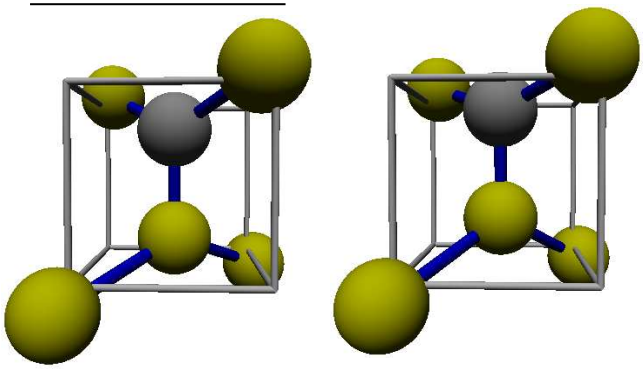

Si-C-Si bond angle → 180 °
⇒ *sp* hybridization

Si-Si-Si bond angle → 120 °
⇒ sp^2 hybridization

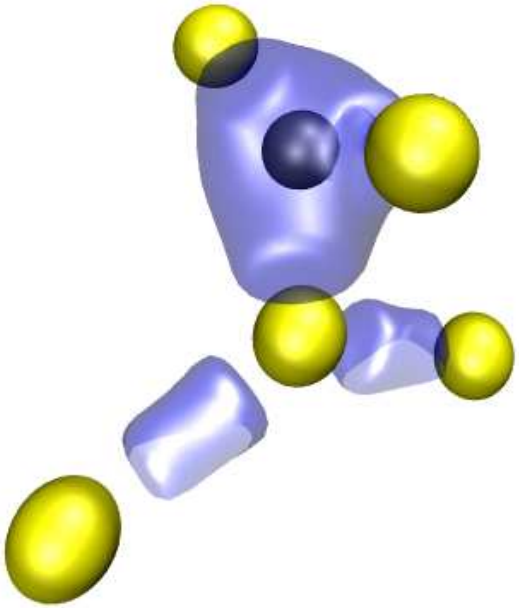

Charge density isosurface

Bond-centered interstitial

- Linear Si-C-Si bond
- Si: one C & 3 Si neighbours
- Spin polarized calculations
- No saddle point!
  Real local minimum!

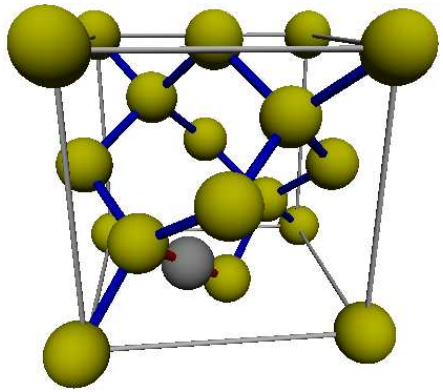

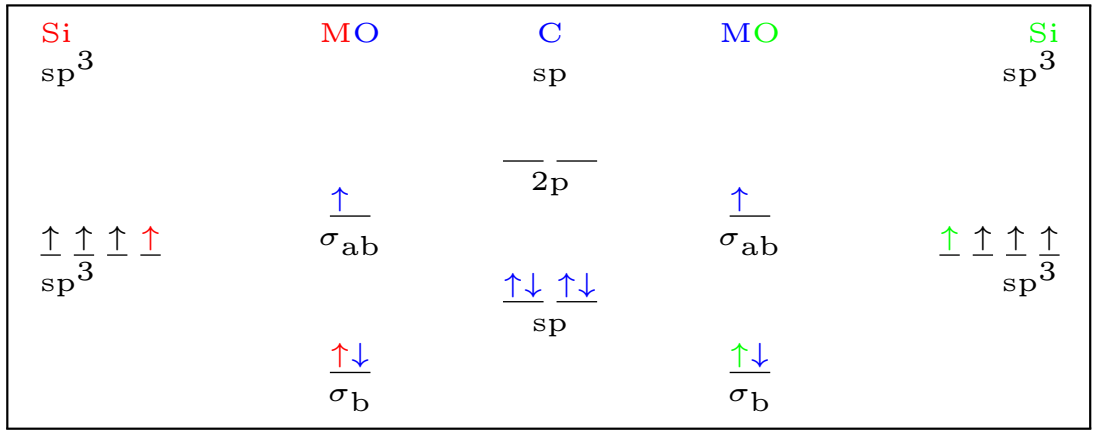

Charge density

- Spin up
- Spin down
- Resulting spin up
- Si atoms
- C atom

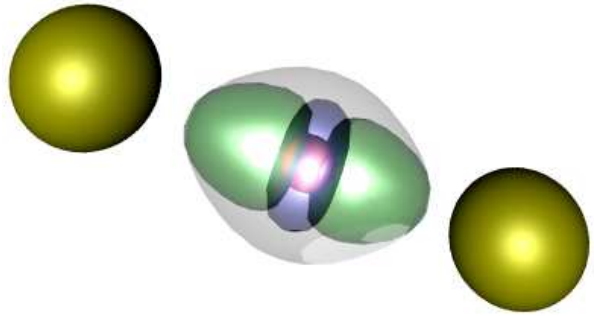

C interstitial migration — ab initio

$[0\,0\,\bar{1}] \rightarrow [0\,0\,1]$

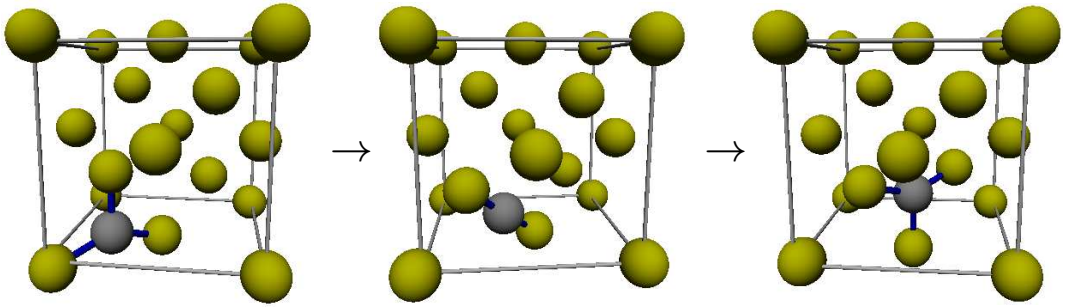

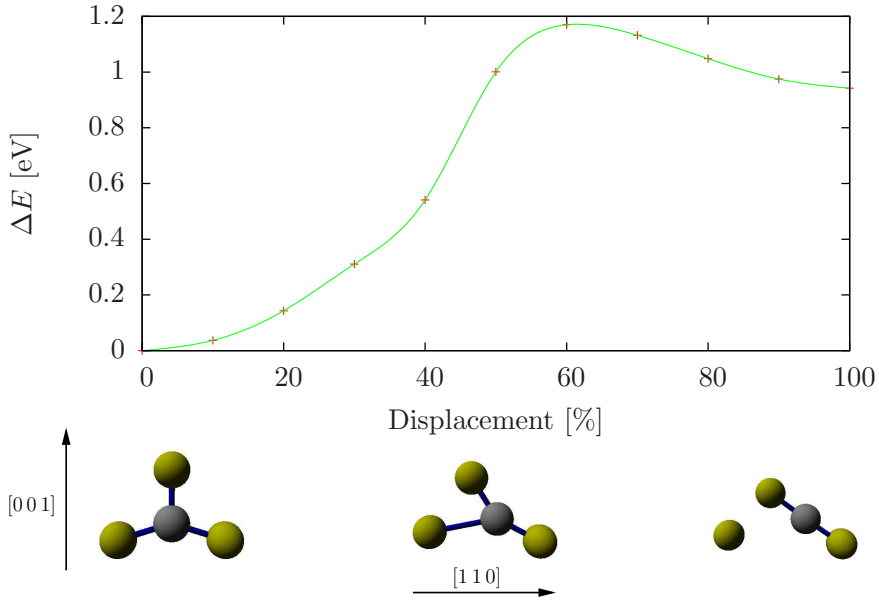

Spin polarization

⇒ BC configuration constitutes local minimum

⇒ Migration barrier to reach BC | $\Delta E = 1.2\,\mathrm{eV}$

$[0\,0\,\bar{1}] \rightarrow [0\,\bar{1}\,0]$

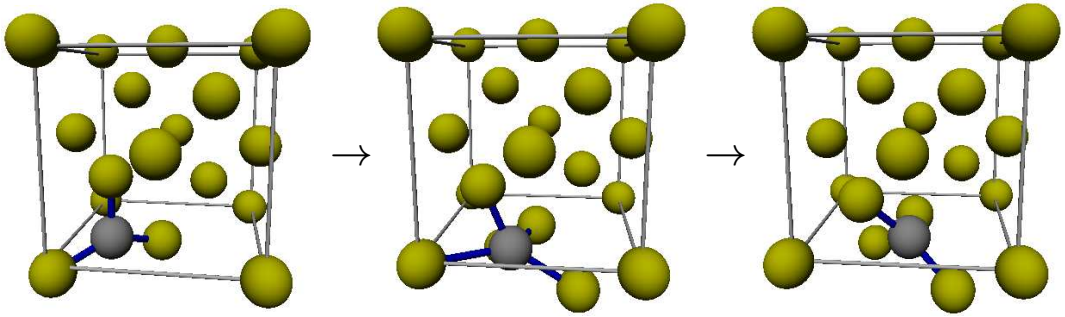

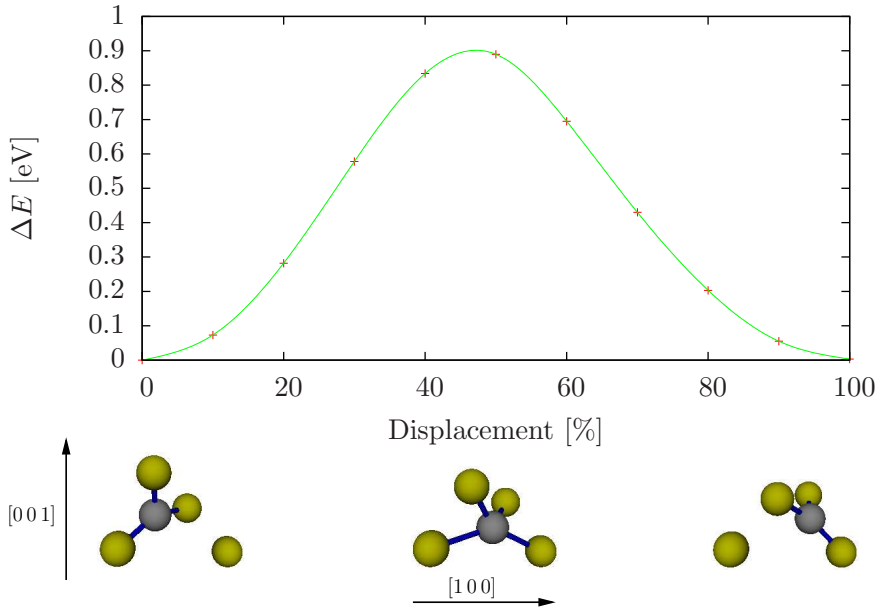

$\Delta E = 0.9\,\mathrm{eV}$ | Experimental values: 0.70–0.87 eV

⇒ Migration mechanism identified!

Note: Change in orientation

Reorientation pathway composed of two consecutive processes of the above type

C interstitial migration — analytical potential

BC to $[0\,0\,\bar{1}]$ transition

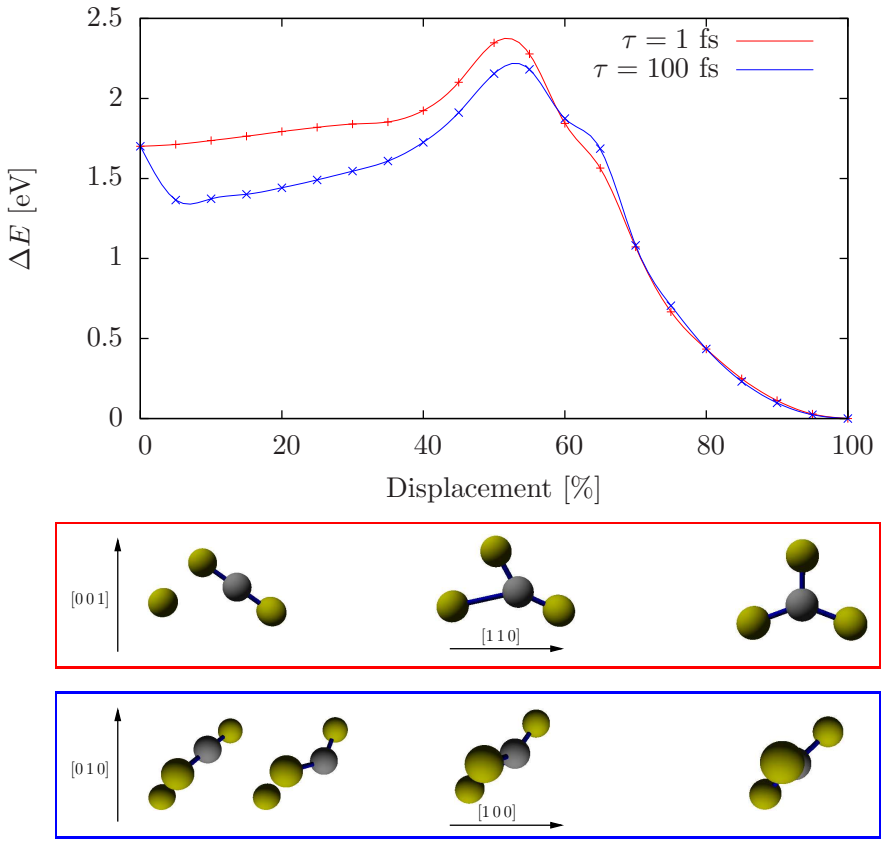

- Lowermost migration barrier
- $\Delta E \approx 2.2\,\mathrm{eV}$
- 2.4 times higher than ab initio result
- Different pathway

Transition involving a $\langle 1\,1\,0 \rangle$ configuration

- Bond-centered configuration unstable
  $\rightarrow$ C_i $\langle 1\,1\,0 \rangle$ dumbbell
- Minima of the $[0\,0\,\bar{1}]$ to $[0\,\bar{1}\,0]$ transition
  $\rightarrow$ C_i $\langle 1\,1\,0 \rangle$ DB

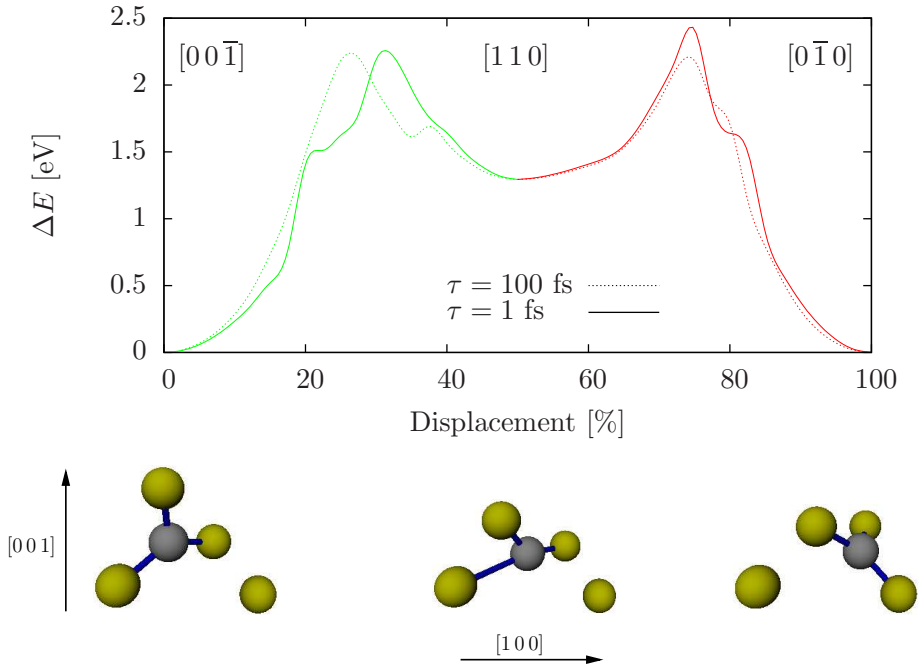

- $\Delta E \approx 2.2\,\mathrm{eV}$ & $0.9\,\mathrm{eV}$
- 2.4 – 3.4 times higher than ab initio result
- After all: Change of the DB orientation

Drastically overestimated diffusion barrier

Defect combinations

Summary of combinations

E_b [eV]	1	2	3	4	5	R
$[0\,0\,\bar{1}]$	-0.08	-1.15	-0.08	0.04	-1.66	-0.19
$[0\,0\,1]$	0.34	0.004	-2.05	0.26	-1.53	-0.19
$[0\,\bar{1}\,0]$	-2.39	-0.17	-0.10	-0.27	-1.88	-0.05
$[0\,1\,0]$	-2.25	-1.90	-2.25	-0.12	-1.38	-0.06
$[\bar{1}\,0\,0]$	-2.39	-0.36	-2.25	-0.12	-1.88	-0.05
$[1\,0\,0]$	-2.25	-2.16	-0.10	-0.27	-1.38	-0.06
C_{sub}	0.26	-0.51	-0.93	-0.15	0.49	-0.05
Vacancy	-5.39 ($\rightarrow C_{sub}$)	-0.59	-3.14	-0.54	-0.50	-0.31

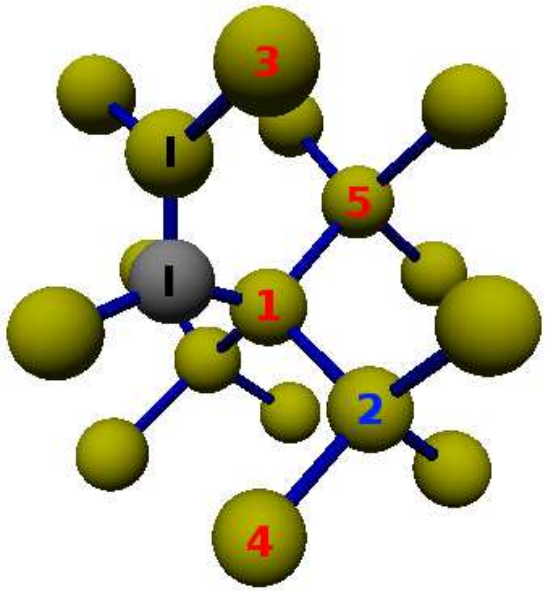

E_b explainable by stress compensation / increase

Combinations of $\langle 1\,0\,0\rangle$-type interstitials

$[1\,0\,0]$ at position 1

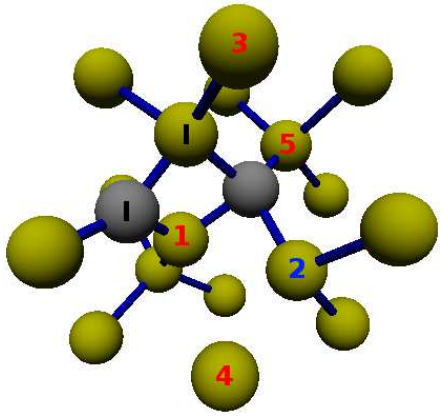

$[0\,\bar{1}\,0]$ at position 1

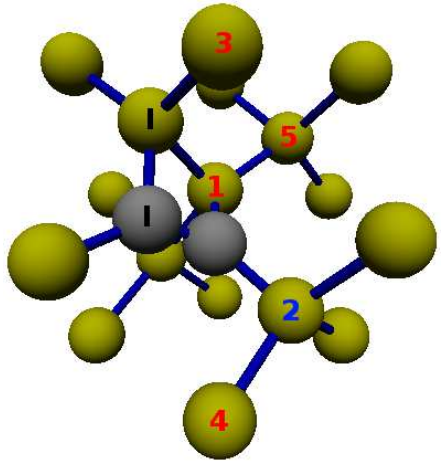

- C_i agglomeration energetically favorable
- Most favorable: C clustering

  However ...

  ... high migration barrier ($> 4\,eV$)

  ... entropy: $4 \times [-2.25]$ versus $2 \times [-2.39]$

C_i agglomeration / no C clustering

Defect combinations

Summary of combinations

E_b [eV]	1	2	3	4	5	R
$[0\,0\,\bar{1}]$						
$[0\,0\,1]$						
$[0\,\bar{1}\,0]$						
$[0\,1\,0]$						
$[\bar{1}\,0\,0]$						
$[1\,0\,0]$						
C_{sub}						
Vacancy	-5.39					

E_b expl

Combinations

[1 0 0] at position

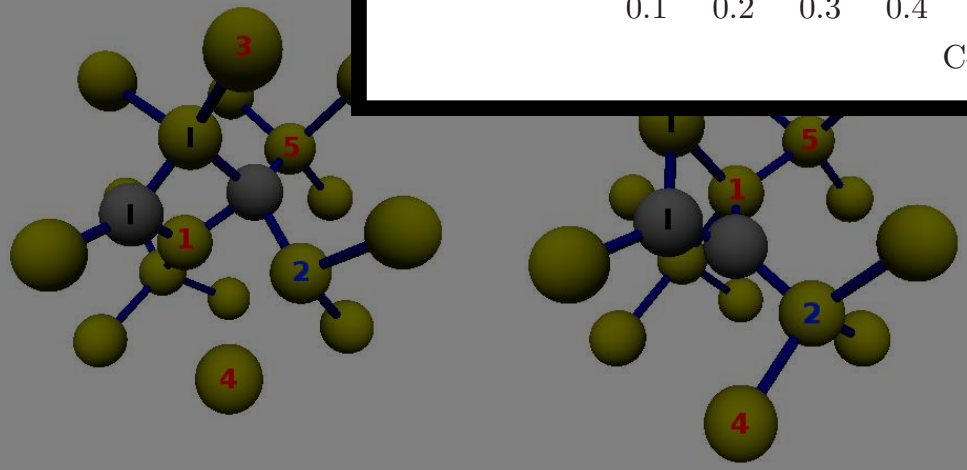

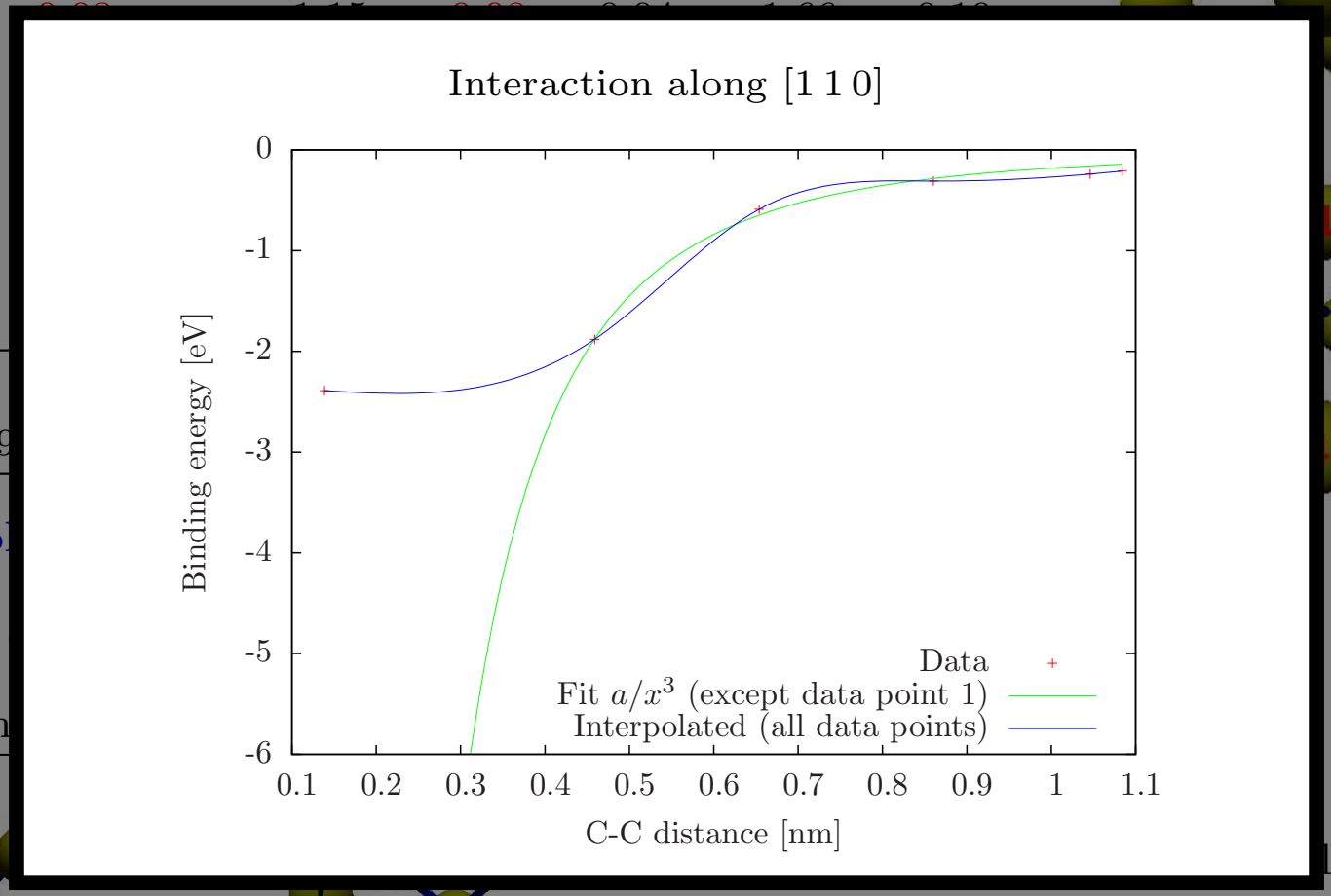

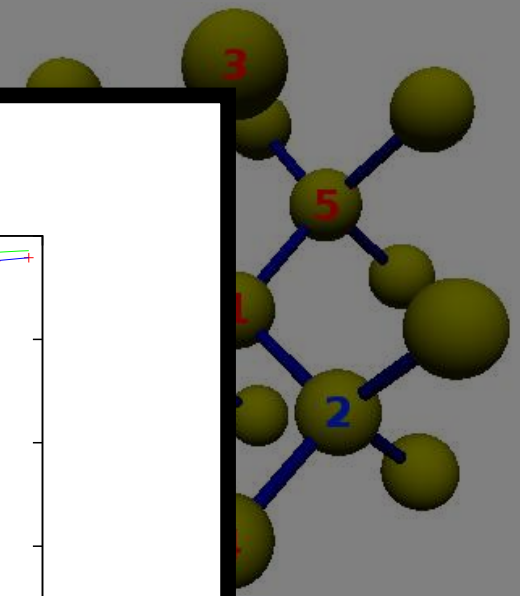

ly favorable

- Most favorable: C clustering

  However ...

  ... high migration barrier ($> 4\,eV$)

  ... entropy: $4 \times [-2.25]$ versus $2 \times [-2.39]$

C_i agglomeration / no C clustering

Defect combinations of C-Si dimers and vacancies

V at 2: $E_b = -0.59$ eV

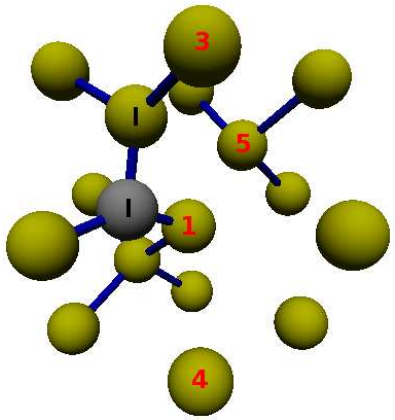

IBS: Impinging C creates V & far away Si_i

Low migration barrier towards C_{sub}

&

High barrier for reverse process

High probability of stable C_{sub} configuration

V at 3, $E_b = -3.14$ eV

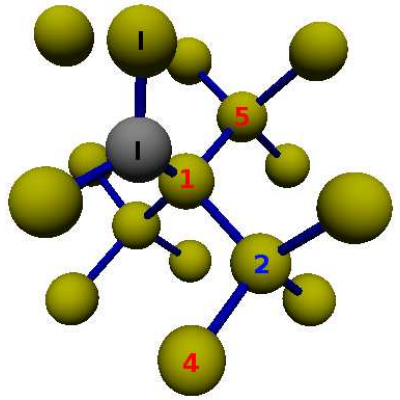

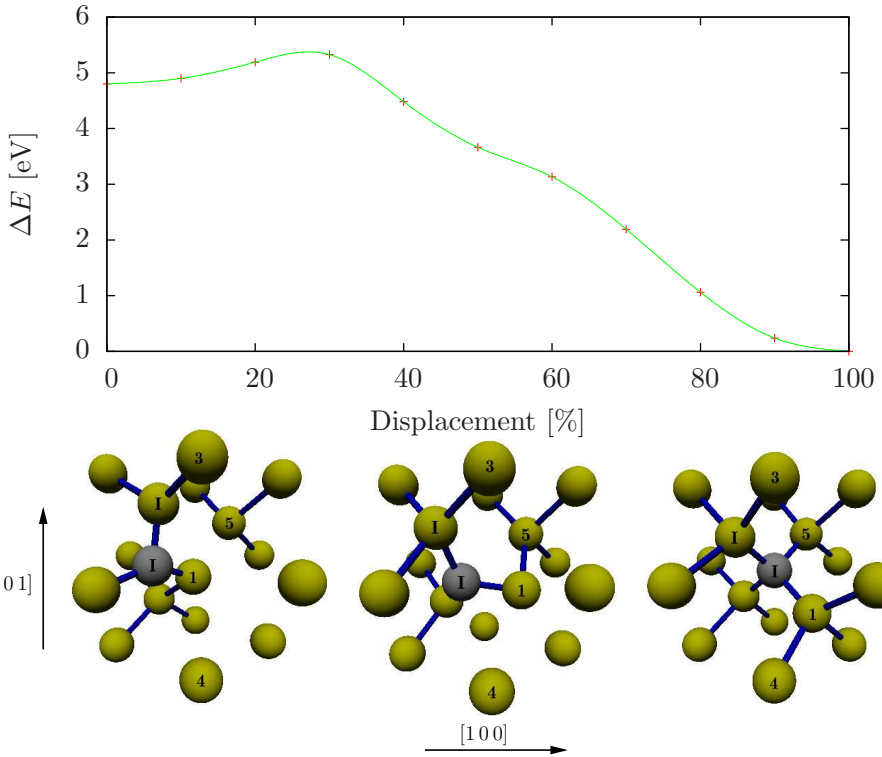

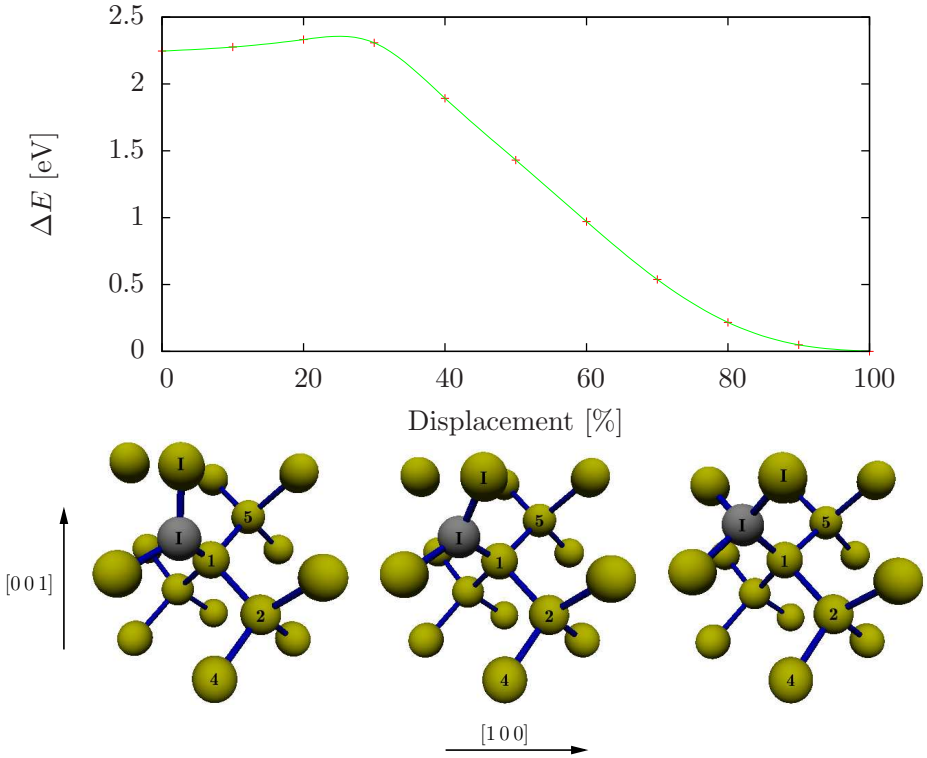

Combinations of substitutional C and Si self-interstitials

C_{sub} - Si_i $\langle 1\,1\,0\rangle$ interaction

- Most favorable: C_{sub} along $\langle 1\,1\,0\rangle$ chain of Si_i
- Less favorable than ground-state C_i $\langle 1\,0\,0\rangle$ DB
- Interaction drops quickly to zero
  $\rightarrow$ low capture radius

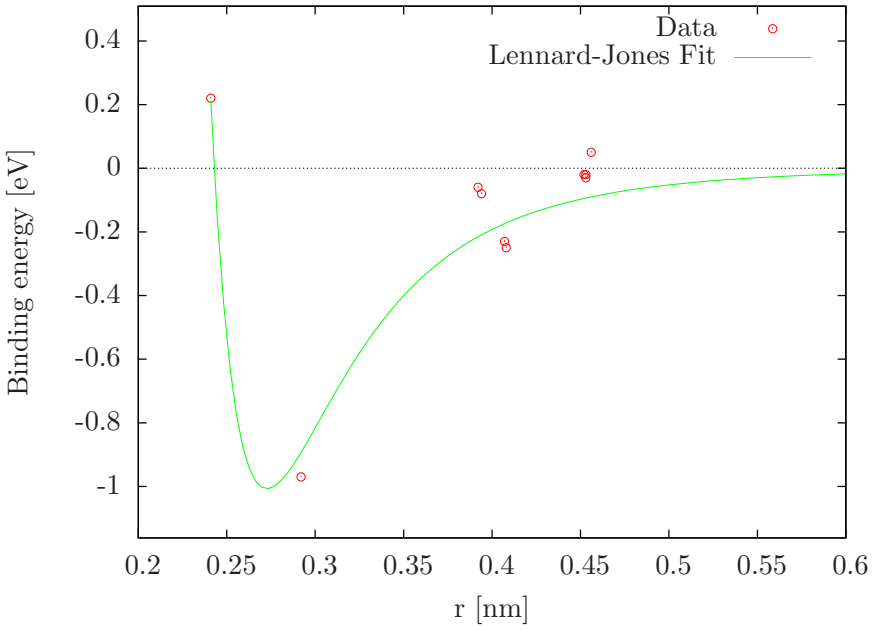

Transition from the ground state

- Low transition barrier
- Barrier smaller than C_i migration barrier
- Low Si_i migration barrier (0.67 eV)
  $\rightarrow$ Separation of C_{sub} & Si_i most probable

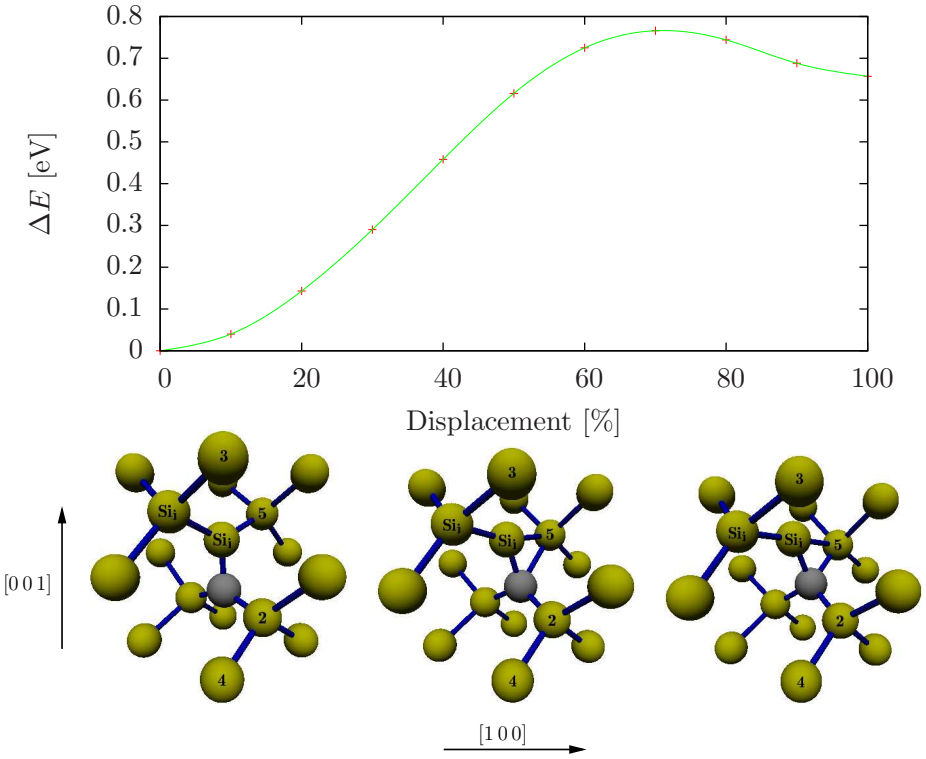

C_{sub} & Si_i instead of thermodynamic ground state

IBS — process far from equilibrium

Combinations of substitutional C and Si self-interstitials

C_{sub} - Si_i $\langle 1\,1\,0\rangle$ interaction

- Most favorable: C_{sub} along $\langle 1\,1\,0\rangle$ chain of Si_i
- Less favorable than ground-state C_i $\langle 1\,0\,0\rangle$ DB
- I

Transition from the ground state

- Low transition barrier
- Barrier smaller than C_i migration barrier

Ab initio MD at 900 °C

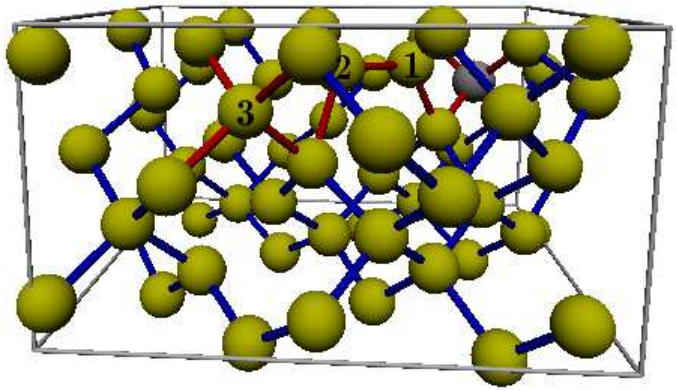

$t = 2230$ fs

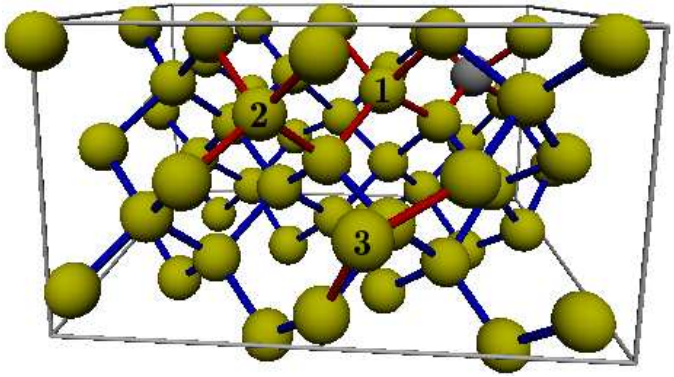

$t = 2900$ fs

Contribution of entropy to structural formation

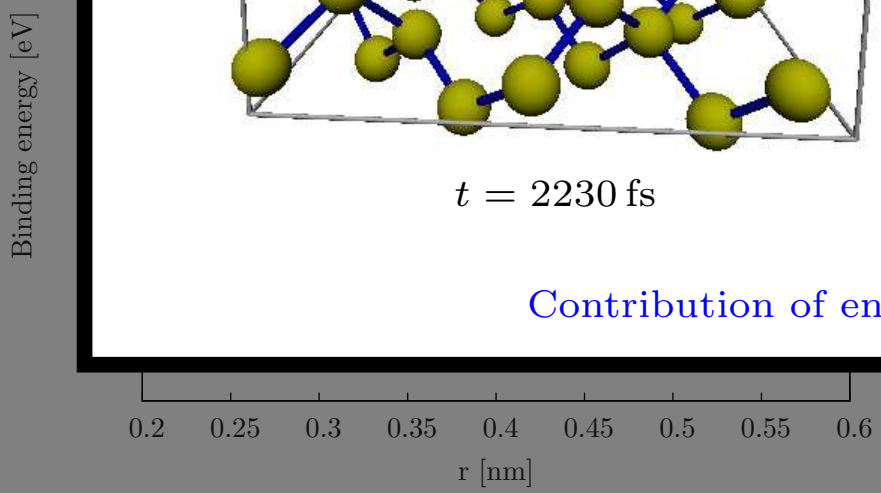

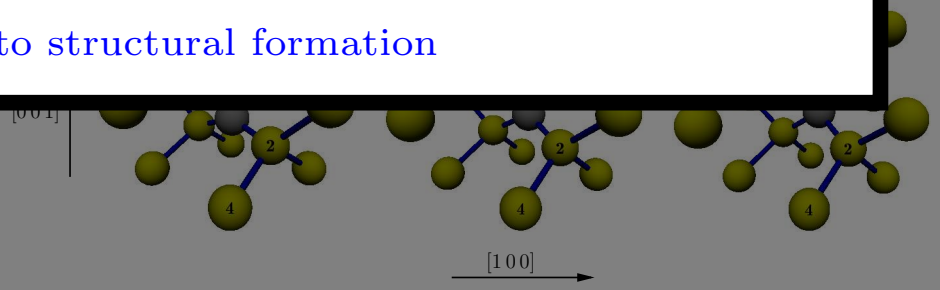

C_{sub} & Si_i instead of thermodynamic ground state

IBS — process far from equilibrium

Silicon carbide precipitation simulations

Procedure

- Create c-Si volume
- Periodc boundary conditions
- Set requested T and $p = 0$ bar
- Equilibration of E_{kin} and E_{pot}

Insertion of C atoms at constant T

- total simulation volume
- volume of minimal SiC precipitate size
- volume consisting of Si atoms to form a minimal precipitate

Run for 100 ps followed by cooling down to 20 °C

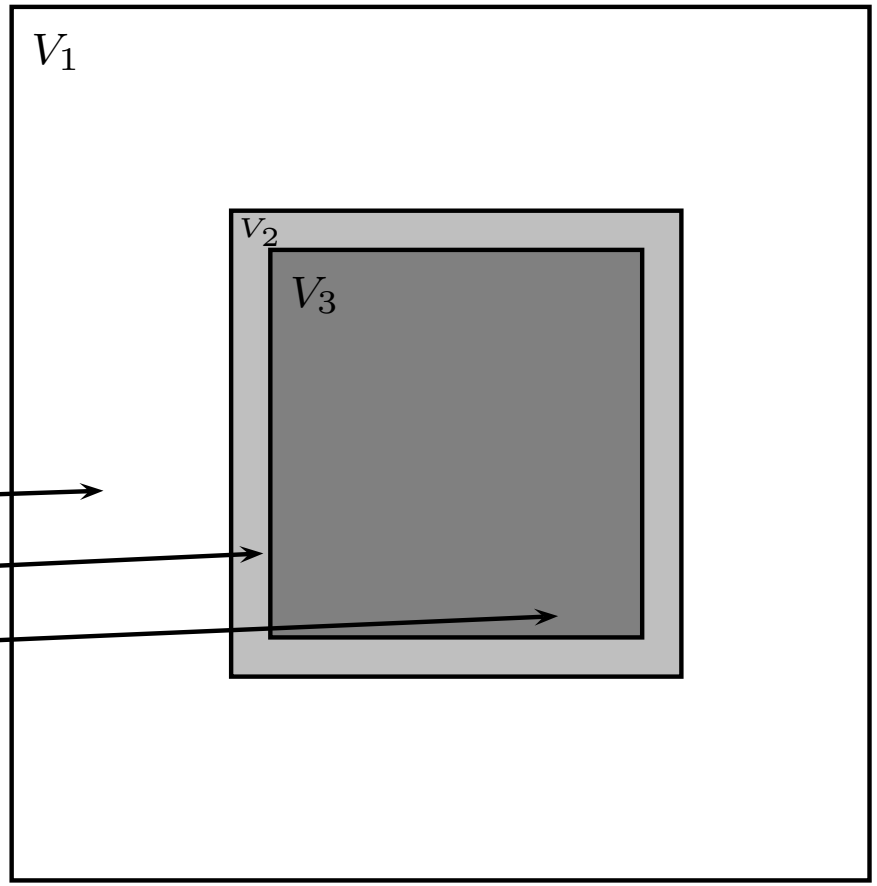

Note

- Amount of C atoms: 6000
  ($r_{\mathrm{prec}} \approx 3.1$ nm, IBS: 2–4 nm)
- Simulation volume: 31^3 Si unit cells
  (238328 Si atoms)

Restricted to classical potential caclulations
→ Low C diffusion / overestimated barrier
→ Consider V_2 and V_3

Silicon carbide precipitation simulations at 450 °C as in IBS

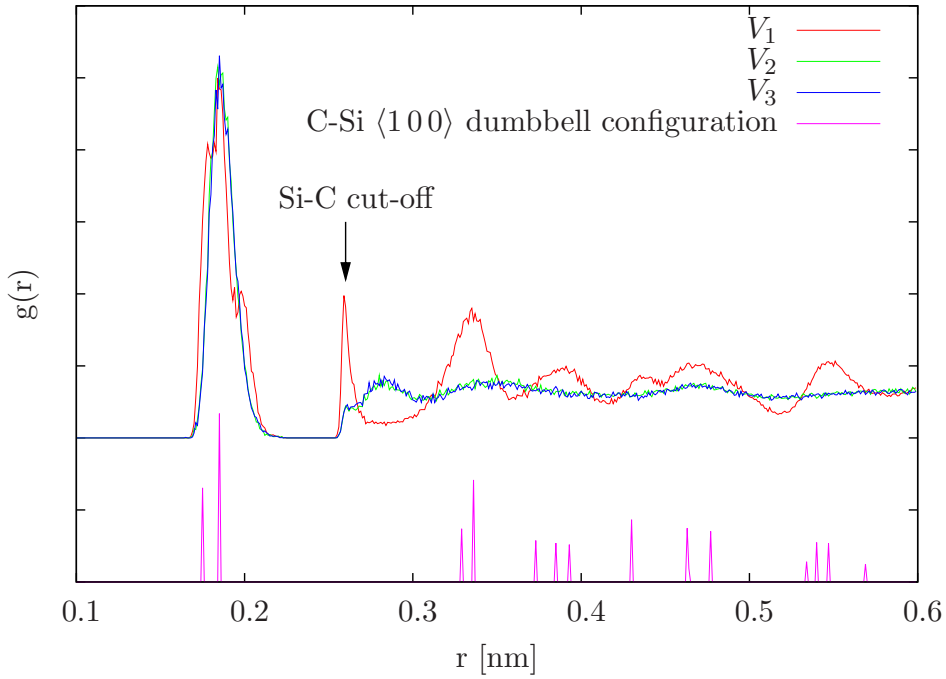

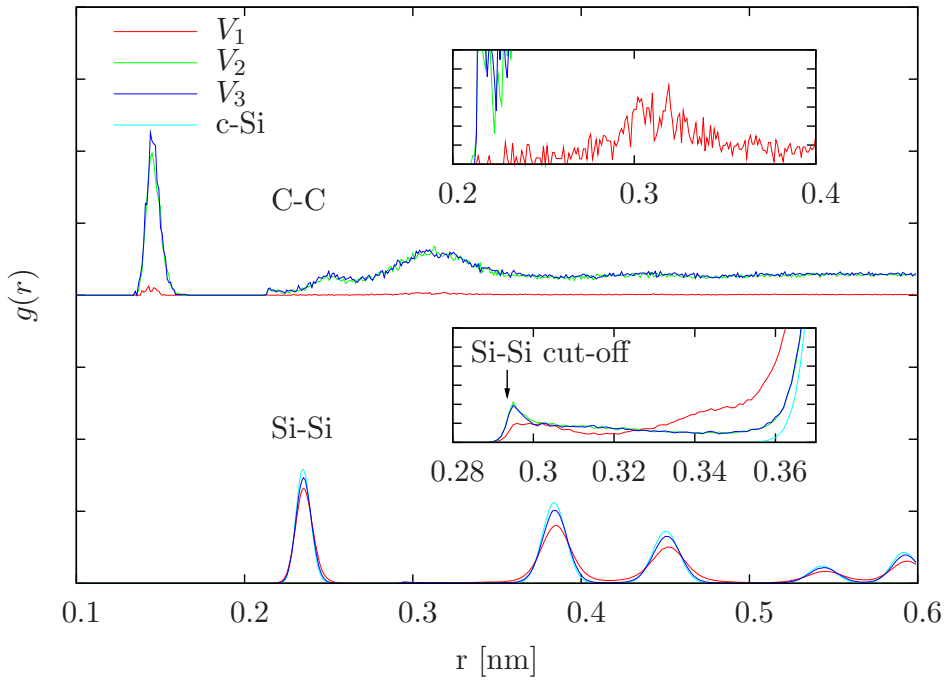

Low C concentration — V_1

⟨1 0 0⟩ C-Si dumbbell dominated structure

- Si-C bumbs around 0.19 nm
- C-C peak at 0.31 nm (expected in 3C-SiC): concatenated differently oriented C_i DBs
- Si-Si NN distance stretched to 0.3 nm

Formation of C_i dumbbells
C atoms in proper 3C-SiC distance first

High C concentration — V_2/V_3

- High amount of strongly bound C-C bonds
- Increased defect & damage density
  → Arrangements hard to categorize and trace
- Only short range order observable

Amorphous SiC-like phase

Silicon carbide precipitation simulations at 450 °C as in IBS

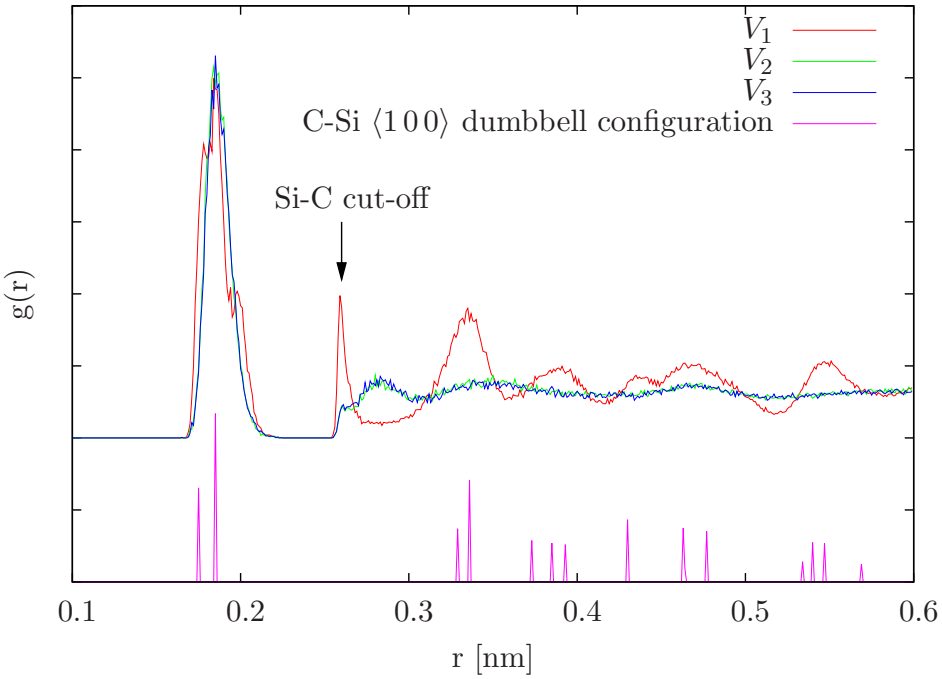

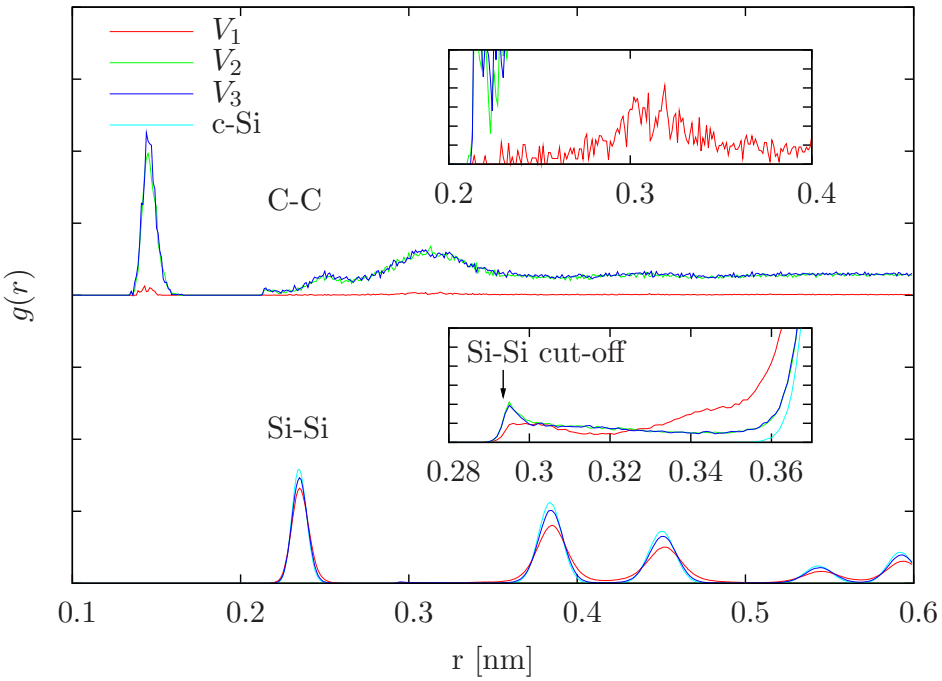

Low C concentration — V_1

⟨1 0 0⟩ C-Si dumbbell dominated structure

- Si-C bumbs around 0.19 nm
- C-C peak at 0.31 nm (expected in 3C-SiC): concatenated differently oriented C_i DBs
- Si-Si NN distance stretched to 0.3 nm

Formation of C_i dumbbells
C atoms in proper 3C-SiC distance first

High C concentration — V_2/V_3

- High amount of strongly bound C-C bonds
- Increased defect & damage density
  → Arrangements hard to categorize and trace
- Only short range order observable

Amorphous SiC-like phase

3C-SiC formation fails to appear

V_1: Formation of C_i indeed occurs
Agglomeration not observed

$V_{2,3}$: Amorphous SiC-like structure
(not expected at 450 °C)
No rearrangement/transition into 3C-SiC

Limitations of MD and short range potentials

Time scale problem of MD

Precise integration & thermodynamic sampling
$\Rightarrow \Delta t \ll (\max \omega)^{-1}$, ω: vibrational mode
$\Rightarrow$ Slow phase space propagation

retain proper thermodynamic sampling

Several local minima separated by large energy barriers
$\Rightarrow$ Transition event corresponds to a multiple of vibrational periods
$\Rightarrow$ Phase transition consists of many infrequent transition events

Accelerated methods: Temperature accelerated MD (TAD), self-guided MD ...

Limitations related to the short range potential

Cut-off function limits interaction to next neighbours
$\Rightarrow$ Overestimated unphysical high forces of next neighbours (factor: 2.4–3.4)

Potential enhanced slow phase space propagation

IBS

3C-SiC also observed for higher T

Higher T inside sample

Structural evolution vs. equilibrium properties

Approach to the (twofold) problem

Increased temperature simulations without TAD corrections
Accelerated methods or higher time scales exclusively not sufficient!

Increased temperature simulations — V_1

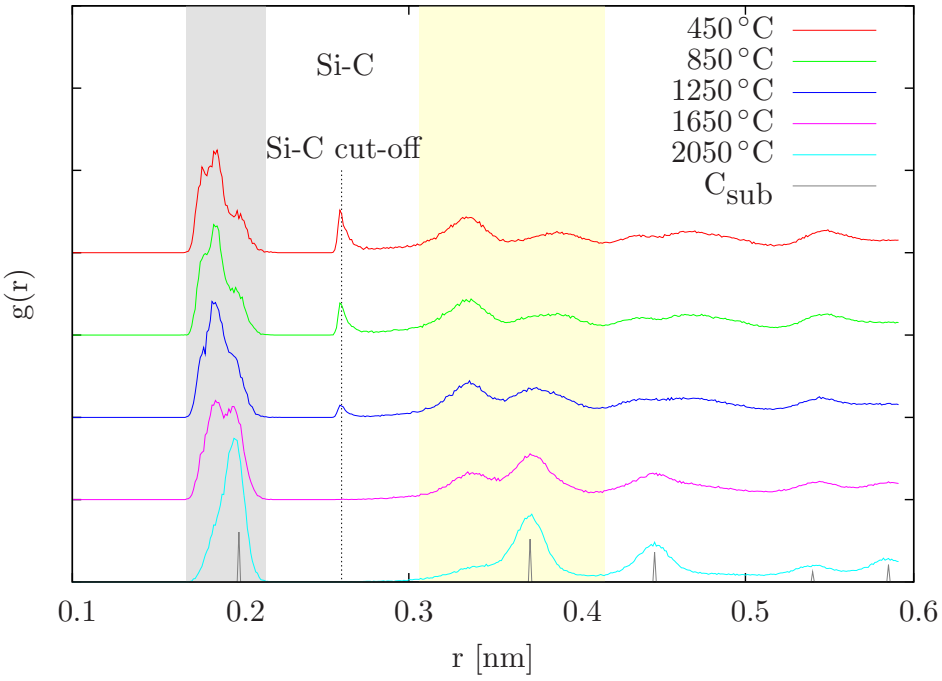

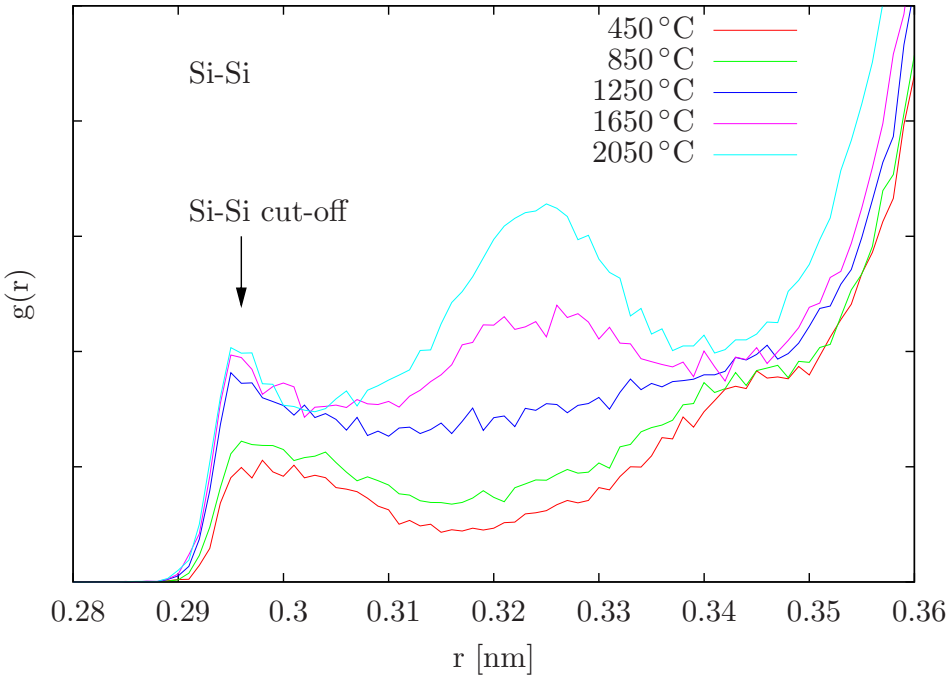

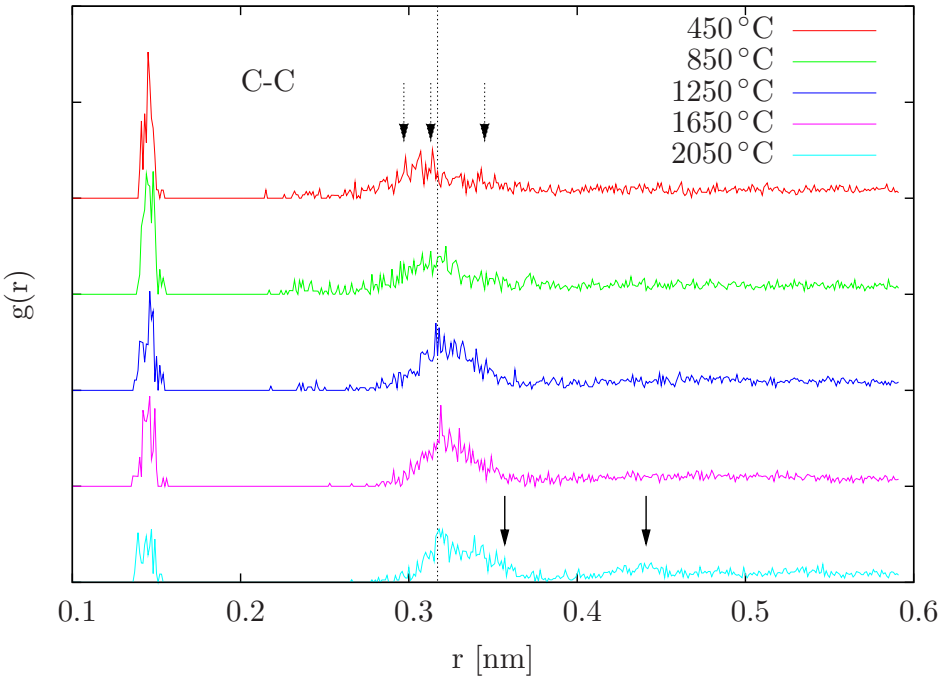

Si-C bonds:

- Vanishing cut-off artifact (above 1650 °C)
- Structural change: C-Si $\langle 1\,0\,0 \rangle \rightarrow C_{sub}$

Si-Si bonds: Si-C_{sub}-Si along $\langle 1\,1\,0 \rangle$ ($\rightarrow$ 0.325 nm)

C-C bonds:

- C-C next neighbour pairs reduced (mandatory)
- Peak at 0.3 nm slightly shifted
  - C-Si $\langle 1\,0\,0 \rangle$ combinations (dashed arrows) $\rightarrow$ C-Si $\langle 1\,0\,0 \rangle$ & C_{sub} combinations (|) $\rightarrow$ pure C_{sub} combinations ($\downarrow$)
  - Range [|-$\downarrow$]: C_{sub} & C_{sub} with nearby Si_I

Increased temperature simulations — V_1

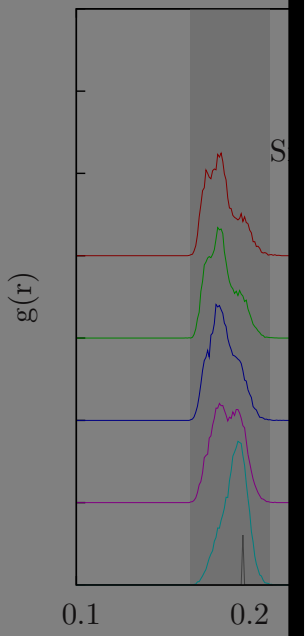

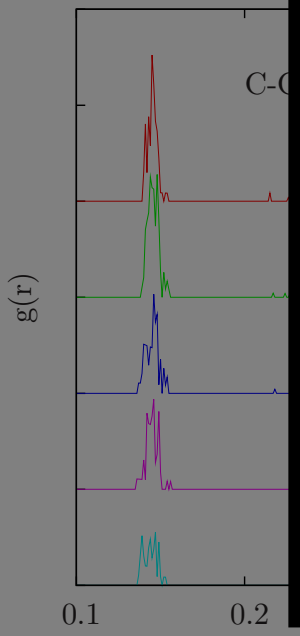

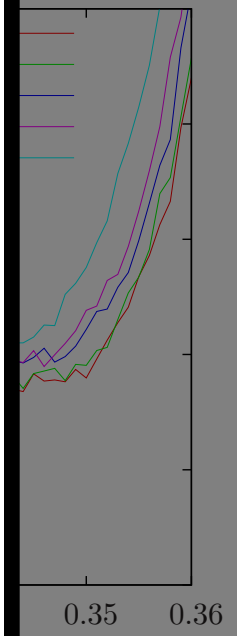

Conclusions on SiC precipitation

C_i — vs — C_{sub}

- Stretched coherent SiC structures
  ⇒ Precipitation process involves C_{sub}
- Explains annealing behavior of high/low T C implantations
  - Low T: highly mobile C_i
  - High T: stable configurations of C_{sub}
- Role of Si_i
  - Vehicle to rearrange C_{sub}— [C_{sub} & $Si_i \leftrightarrow C_i$]
  - Building block for surrounding Si host & further SiC
  - Strain compensation . . .
    . . . Si/SiC interface
    . . . within stretched coherent SiC structure

Precipitation mechanism involving C_{sub}
High T ↔ IBS conditions far from equilibrium

50 °C)

sub

0.325 nm)

nandatory)

ed arrows)

tions (|)

- Range [|-↓]: C_{sub} & C_{sub} with nearby Si_I

Summary / Outlook

Diploma thesis

Monte Carlo simulation modeling the selforganization process

leading to periodic arrays of nanometric amorphous SiC precipitates

Doctoral studies

Classical potential molecular dynamics simulations ...

Density functional theory calculations ...

...on defect formation and SiC precipitation in Si

How to proceed ...

MC → empirical potential MD → Ground-state DFT ...

... beyond LDA/GGA methods & ground-state DFT

Investigation of structure & structural evolution ...

... electronic/optical properties

... electronic correlations

... non-equilibrium systems

Acknowledgements

Thanks to ...

Augsburg

- Prof. B. Stritzker (accomodation at EP IV)
- Ralf Utermann (EDV)

Helsinki

- Prof. K. Nordlund (MD)

Munich

- Bayerische Forschungsstiftung (financial support)

Paderborn

- Prof. J. Lindner (SiC)
- Prof. G. Schmidt (DFT + financial support)
- Dr. E. Rauls (DFT + SiC)

Stuttgart

Thank you for your attention / invitation!